PHILOSOPHICAL TRANSACTIONS OF THE ROYAL SOCIETY A MATHEMATICAL, PHYSICAL & ENGINEERING SCIENCES

Rotational Analysis of the 2600 angstrom Absorption System of Benzene

J. H. Callomon, T. M. Dunn and I. M. Mills

Phil. Trans. R. Soc. Lond. A 1966 **259**, 499-532
doi: 10.1098/rsta.1966.0023

ROTATIONAL ANALYSIS OF THE 2600 Å ABSORPTION SYSTEM OF BENZENE

By J. H. CALLOMON, T. M. DUNN and I. M. MILLS
University College, London; University of Michigan, Ann Arbor, Mich.; and the University of Reading

(*Communicated by H. C. Longuet-Higgins, F.R.S.—Received* 14 *June* 1965)

[Plates 7 to 10]

CONTENTS

The 2600Å absorption system of benzene has been examined with very high resolving power, and the rotational fine structure partially analysed by comparison with computed contours.

Vibronic bands involving degenerate e_{2g} vibrations have contours characteristic of the vibrational angular momentum, and Coriolis coefficients ζ have been determined for the lowest e_{2g} vibrations in ground and B_{2u} excited states. Band contours thus provide an additional criterion for checking vibrational assignments. In particular, values of ζ determine the separation between band maximum and origin which can thus be calculated, and the vibrational analysis consequently refined in certainty and precision. Improved values of several fundamentals have been obtained, some new vibrational assignments made, and some previous ones rejected. Some important anharmonic constants have also been obtained. Vibronic relative intensities are briefly discussed.

The rotational and vibrational evidence together make it certain that the equilibrium configurations of the carbon skeleton in benzene are exactly planar and hexagonal in both the ground and excited states, point group D_{6h}. The rotational constants then give an estimate of the increase in C—C distance on excitation of $+0{\cdot}038$ Å, in excellent agreement with estimates from other sources. The electronic origin of the system is revised: $T_{00} = 38086{\cdot}1$ cm^{-1}.

1. Introduction

The ultraviolet spectrum of benzene has been much studied in the last thirty years, but so far only one paper has appeared on the spectrum under high resolution (Turkevich & Fred 1942). The great interest in benzene lies in the important role which it plays in electronic

Vol. 259. A. 1104. (Price 18*s*. 6*d*.; U.S. $2.75) 60 [Published 19 May 1966

theories of chemical structure, and there have been many papers dealing with the assignment of its excited electronic states and calculation of their energies. Theoreticians, at least, are united in assigning the lowest singlet transition as $^1B_{2u}$–$^1A_{1g}$ and since Sklar's original identification of this transition with the 2600 Å system there has been no serious evidence to the contrary.

TABLE 1. SYMMETRY SPECIES, SELECTED CHARACTERS, NOTATION OF NORMAL COORDINATES Q, AND FUNDAMENTAL FREQUENCIES OF BENZENE, GROUND STATE

					$Q_j^{(3)}$		fundamentals (cm^{-1})[4]	
D_{6h}	$2C_6(z)$	σ_h[1]	$C_2(y)$	activity[2]	W.D.C., this work	H.	C_6H_6	C_6D_6
a_{1g}	+1	+1	+1	R($\alpha_{x^2+y^2}$, α_{z^2})	1	2	995·4[5]	945·6[5]
					2	1	3073	2303
a_{2g}	+1	+1	−1	—	3	3	1350	1059
b_{1g}	−1	−1	+1	—	—	—	—	—
b_{2g}	−1	−1	−1	—	4	8	707	599
					5	7	990	829
e_{2g}	−1	+2	0	R($\alpha_{x^2-y^2}$, α_{xy}) $\Sigma\zeta = 0$	6	18	608·0[5]	580·2[5]
					7	15	3056	2274
					8	16	1596[6]	1558
					9	17	1178	869
e_{1g}	+1	−2	0	R(α_{xz}, α_{yz})	10	11	846	660
a_{1u}	+1	−1	+1	—	—	—	—	—
a_{2u}	+1	−1	−1	i.r.(T_z, ∥)	11	4	674·0[7]	496·2[7]
b_{1u}	−1	+1	+1	—	12	6	1010	970
					13	5	3057	2285
b_{2u}	−1	+1	−1	—	14	9	1309	1282
					15	10	1146	824
e_{2u}	−1	−2	0	—	16	20	398·6[5]	347·4[5]
					17	19	967	787
e_{1u}	+1	+2	0	i.r.($T_{x,y}$, ⊥) $\Sigma\zeta = -1$	18	14	1037	814
					19	13	1482	1333
					20	12	3064	2288

(1) +, displacements in-plane; −, displacements out of plane.
(2) R, Raman, i.r., infrared.
(3) W.D.C., Wilson, Decius & Cross (1955); H., Herzberg (1945).
(4) Values after Brodersen & Langseth (1956); from vapour phase data.
(5) From the ultraviolet spectrum, determined here.
(6) As (4), corrected for Fermi resonance.
(7) High resolution infrared values, after Danti & Lord (1958).

It is necessary briefly to review the experimental evidence for the assignment since it is of importance in what follows. The evidence is of two types: the vibrational structure of the vapour spectrum; and certain features of the spectrum of the crystal at low temperatures, which will be mentioned only briefly. A complete discussion up to 1948 can be found in paper I of Ingold and co-workers' series of that year (Best, Garforth, Ingold, Poole & Wilson 1948). In this series they tested and extended the vibrational analysis originally put forward by Sklar (1937) and later discussed in more detail by Sponer, Nordheim, Sklar & Teller (1939) and Sponer (1940) by examining deuterium-substituted benzenes.

The electric dipole selection rules for hexagonal benzene allow only the two types of transition, E_{1u}–A_{1g} (perpendicular) and A_{2u}–A_{1g} (parallel), table 1, and Sklar's suggestion that vibrations of e_{2g} symmetry mix the $^1B_{2u}$ state with a higher $^1E_{1u}$ state (presumably the one connected to the ground state by the very intense transition near 1850 Å), thus allowing the transition to appear, was supported on a vibrational basis both by Sponer *et al.* and Ingold *et al.* The vibration most effective in causing the mixing was identified by Sklar as the one giving the 606 cm^{-1} frequency found in the Raman spectrum of the liquid.

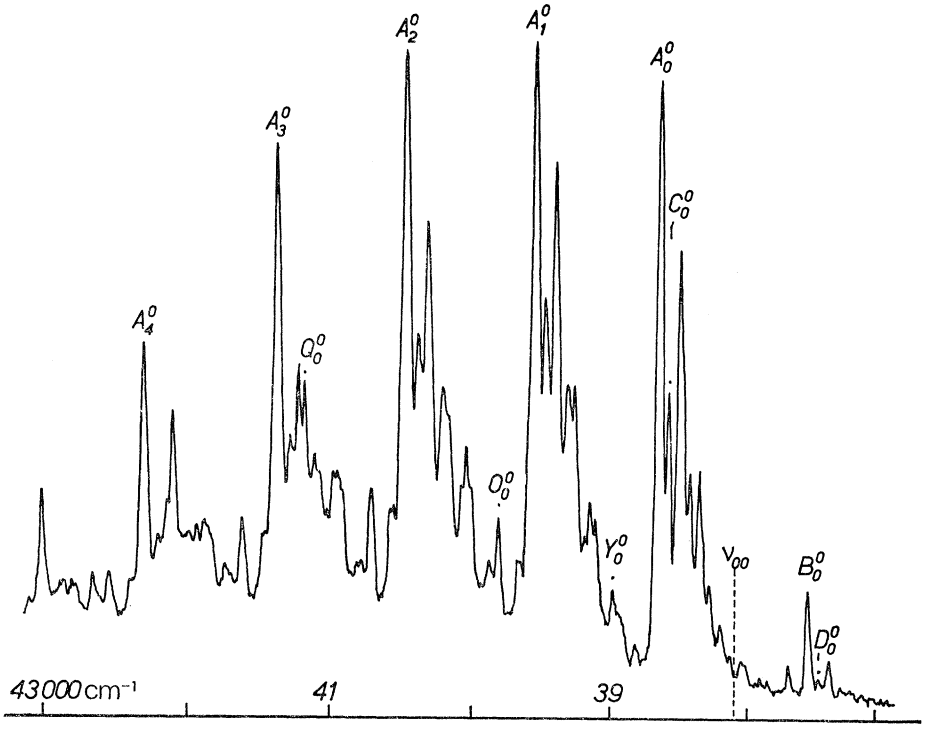

FIGURE 1. Absorption spectrum of benzene vapour under low resolution.

The low resolution vapour spectrum of benzene is shown in figure 1 and the basic energy level scheme is shown in figure 2. The electronic origin (0, 0) band does not appear, and the spectrum may be regarded as based, in the main, on two 'false' vibronic origins: band A_0^0, 6_0^1, transition from the zero level of the ground state to the level of the first quantum of ν_6' (e_{2g}, 522 cm^{-1}) in the excited state; and band B_0^0, 6_1^0, from the first quantum of ν_6'' (e_{2g}, 608 cm^{-1}) in the ground state to the zero level of the excited state. B_0^0 is a hot band in absorption, weaker than A_0^0 in about the ratio of a Boltzmann factor corresponding to 608 cm^{-1}. Built on these two vibronic origins, the rest of the spectrum consists of progressions in the totally symmetric vibrations, and 1–1, 2–2, ..., n–n sequences of thermally accessible vibrations, which in benzene are almost all non-totally symmetrical.

Besides the stronger bands assigned as above, there are numerous weaker ones based on additional vibronic origins. Benzene has four fundamentals of species e_{2g}, with frequencies 608, 1178, 1596 and 3056 cm^{-1} (C_6H_6, ground state), and it has been claimed that besides 608 cm^{-1}, two of the remaining three also appear in the spectrum, the exception being the 1178 cm^{-1} mode which involves mainly in-plane C—H bending. Finally, in addition to these vibronic origins involving fundamentals, Ingold *et al.* assigned a further six origins

PHILOSOPHICAL TRANSACTIONS OF THE ROYAL SOCIETY A MATHEMATICAL, PHYSICAL & ENGINEERING SCIENCES

arising through two-quantum combinations of non-totally symmetric vibrations. The complete list of possible one- and two-quantum orgins is given in table 2. In none of the previous analyses is there any sign of overall odd-quantum changes in vibrations which are non-totally symmetric in D_{6h} other than those mentioned, of species e_{2g}.

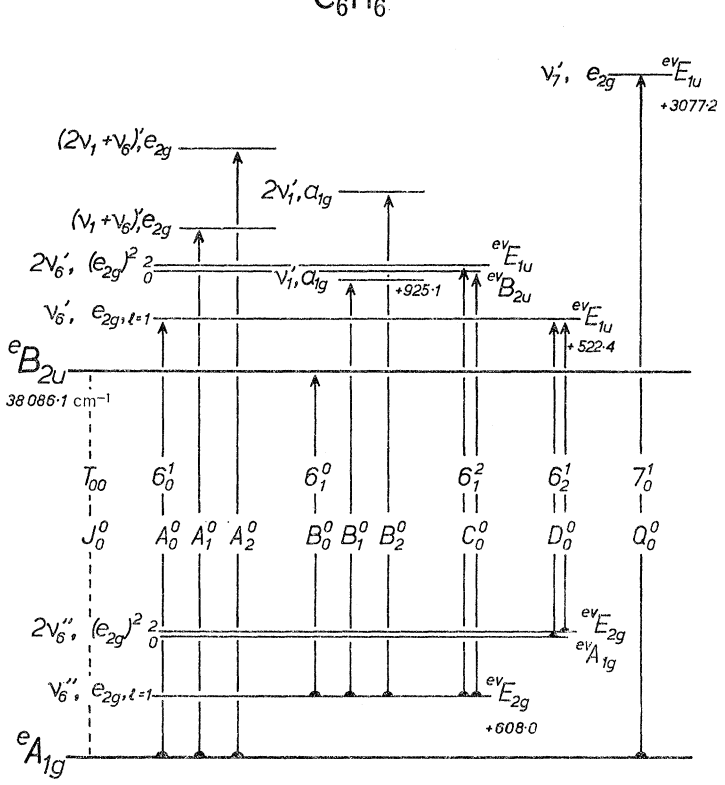

FIGURE 2. Basic vibrational energy level diagram for the 2600 Å absorption system of benzene. The pure electronic transition J_0^0 is absent in the vapour phase spectrum, but is seen weakly in condensed phases.

TABLE 2. SINGLE OR BINARY COMBINATIONS OF VIBRATIONS ν_i, ν_j OF BENZENE CAPABLE OF GENERATING VIBRONIC ORIGINS IN AN ELECTRONIC $^1B_{2u}$–$^1A_{1g}$ TRANSITION

$$\Gamma\langle ev_i'| \times \Gamma|ev_j''\rangle \supset E_{2g}$$

type of transition	vibrational species
	e_{2g}
i_0^1, i_1^0	$(e_{1,2,g,u})^2 = E_{2g}+A_{1g}$
i_0^2, i_1^1, i_2^0	$e_{2g}\times a_{1,2g} = E_{2g}$
$i_0^1 j_0^1, i_0^1 j_1^0, i_1^0 j_1^0$	$e_{2u}\times a_{2u} = E_{2g}$
	$e_{1u}\times b_{1,2u} = E_{2g}$
	$e_{1g}\times b_{2g} = E_{2g}$
	$e_{1g}\times e_{1g} = E_{2g}+A_{1g}+A_{2g}$
	$e_{1u}\times e_{1u} = E_{2g}+A_{1g}+A_{2g}$
	$e_{2g}\times e_{2g} = E_{2g}+A_{1g}+A_{2g}$
	$e_{2u}\times e_{2u} = E_{2g}+A_{1g}+A_{2g}$

Vibrations of species e_{2g} can formally mix an E_{1u} electronic state not only with B_{2u} states but also with B_{1u} states, i.e. $\Gamma(^eB_{1,2u}) \times \Gamma(^ve_{2g}) \supset \Gamma(^{ev}E_{1u})$

(left superscripts e, v and ev referring to electronic, vibrational and vibronic species respectively), so that on the vibrational evidence alone the electronic transition could

equally well be $^1B_{1u}$–$^1A_{1g}$. Conversely, vibronic perturbation leading to spectral activity of electronically forbidden transitions need not be limited to mixing of $B_{1,\,2u}$ with E_{1u}, for there are at least conceivable vibrations capable in principle of mixing them with A_{2u} states (parallel bands):

$$\Gamma(^eB_{1u}) \times \Gamma(^vb_{2g}) \supset \Gamma(^{ev}A_{2u}),$$
$$\Gamma(^eB_{2u}) \times \Gamma(^vb_{1g}) \supset \Gamma(^{ev}A_{2u}).$$

There are bound to be excited $^1A_{2u}$ states, even if only of Rydberg type; and hence a $^eB_{2u}$–$^eA_{1g}$ transition might be expected to show a vibronic origin, however weakly, of parallel bands, based on a b_{1g} fundamental; similarly, for a $^eB_{1u}$–$^eA_{1g}$ transition, on a b_{2g} fundamental. However, benzene has b_{2g} but *no* b_{1g} fundamental modes (table 1); and despite careful search Ingold *et al.* could find no evidence in the spectrum of vibronic origins involving the known b_{2g} fundamentals. They therefore took this as negative evidence that the 2600 Å transition is *not* $^eB_{1u}$–$^eA_{1g}$.

It has also been claimed that the so-called Davydov splitting interval observed in the polarized spectrum of crystalline benzene supports the $^eB_{2u}$–$^eA_{1g}$ assignment (Fox & Schnepp 1955), but the calculations on which the analysis of the crystal spectrum is based contain assumptions which are difficult to justify, and any conclusions from this source must be as yet regarded as tentative. Other arguments based on the polarized crystal spectra of substituted benzenes of symmetries less than D_{6h} are also liable to uncertainty, in that significance of the direction of a transition moment in a crystal is only unambiguous if it can be shown simultaneously and conclusively that the transition is electronically symmetry allowed, and that vibronically induced components are weak and do not arise from crystal forces. This applies even apart from the more dubious assumption that the transition in the substituted benzene can be uniquely correlated with the 2600 Å system of benzene. It may well be that this is so, but it is inadvisable to assume its validity *a priori*.

Thus, the most that can be said up to the present, experimentally, is that if all the vibrational assignments are correct, the upper state of the 2600 Å system is either $^eB_{2u}$ or $^eB_{1u}$ with the former favoured on negative evidence. This choice has not been conclusively resolved by the present study, and in fact a rotational analysis is incapable of resolving it: it can here only distinguish parallel from perpendicular transition moments. It does, however, establish what the vibrational analysis had suggested, that the strong bands of the 2600 Å system are indeed all perpendicular.

1·1. *Molecular geometries*

The evidence of the vibrational analyses has always been wholly consistent with a planar hexagonal equilibrium configuration for benzene, in its excited state as in its ground state, and the same evidence has been used in two ways to estimate the changes in bond lengths that occur on excitation: (i) through a quantitative application of the Franck–Condon principle to the intensity contours of the progressions in the totally symmetric vibrations (Craig 1950*b*); and (ii) with the aid of empirical relations between force constants and bond lengths of the type of Badger's rule (Best *et al.* 1948). The results of the present rotational analysis are also wholly in accord with a planar hexagonal configuration and provide a third estimate of bond-length changes from moments of inertia in excellent agreement with the other two. In contrast, electron spin resonance studies of the lowest excited *triplet* state

of benzene, admittedly in the solid phase, indicate distortions from D_{6h} symmetry (de Groot & van der Waals 1963). Although small distortions from hexagonal symmetry are hard to characterize unambiguously, we believe that the combined evidence from vibrational and rotational analyses leads to the unambiguous conclusion that benzene has D_{6h} symmetry in both the ground and the excited states of the 2600 Å system.

Absolute upper-state dimensions are obtained relative to those of the ground state. The latter are derived from inertial constants measured in the pure rotational Raman spectrum (Stoicheff 1954):

$$B_0(C_6H_6) = 0{\cdot}18960 \pm 0{\cdot}00005\,\mathrm{cm}^{-1}, \quad B_0(C_6D_6) = 0{\cdot}15681 \pm 0{\cdot}00008\,\mathrm{cm}^{-1}.$$

These values have been used in this analysis without change.

1·2. *Vibrational notation*

It has been customary in previous work to label the various bands of the 2600 Å system with letters $A_n^s, B_n^s, \ldots$. Right subscripts denote the number of quanta of the totally symmetric ring 'breathing' vibration excited, $+n$ being used for excited state progressions and $-n$ for groundstate progressions. The superscripts number the members of the sequences in the lowest, e_{2u}, vibration (0,0), (1,1), ... (s,s). Although fairly well established, this notation is in itself cumbersome, not very informative, and not consistently applied to the various deuterated benzenes. There is now a good case for a more systematic notation and this has been used in this paper, with the Sponer–Ingold notation in brackets where this may be helpful.

The notation is as follows: (i) Some particular order of numbering the normal coordinates of ordinary benzene in its ground state is chosen. Of the two conventions in common use we follow that of Wilson (1934; see also Wilson, Decius & Cross 1955), which was also adopted by Crawford & Miller (1949), Whiffen (1955), Brodersen & Langseth (1956), and Albrecht (1960*a*). The other is that of Herzberg (1945), and to avoid confusion the two numberings are shown in table 1 together with the Schoenfliess symmetry symbols and the values of the ground state fundamental frequencies. The same numbering is retained for C_6D_6 and the excited states. (ii) Transitions between vibronic levels involving vibrational excitation are indicated by the numbers of the normal coordinates in which $v \neq 0$ in either state. Superscripts show the number of quanta excited in the upper state, subscripts the number excited in the lower state. Progressional changes ($\Delta v \neq 0$) are given first, followed by sequences. Thus, for example, the bands A_0^0, B_0^0 involve single quanta of what table 1 shows to be ν_6' and ν_6'', and the transitions are written 6_0^1 and 6_1^0, respectively. The lowest frequency (e_{2u}) is ν_{16}, so that the sequence bands A_0^1, B_0^1 are $6_0^1 16_1^1$ and $6_1^0 16_1^1$ respectively. The symmetrical ring breathing frequency (a_{1g}) is ν_1, so that the bands A_1^0, B_1^0 are written $1_0^1 6_0^1$ and $1_0^1 6_1^0$, with their sequences A_1^1, B_1^1 as $1_0^1 6_0^1 16_1^1$ and $1_0^1 6_1^0 16_1^1$. In transitions involving multiple quanta of degenerate vibrations in which there can be more than one component active in the spectrum, the notation can be easily extended to the additional quantum number required to specify the levels, e.g. l. Thus, there are two bands under

$$C_0^0\colon 2\nu_6'({}^vE_{2g}, l=2) - \nu_6''({}^ve_{2g}, l=1) \quad \text{and} \quad 2\nu_6'({}^vA_{1g}, l=0) - \nu_6''({}^ve_{2g}, l=1),$$

written for short as $6_1^2 l_1^2$ and $6_1^2 l_1^0$.

The advantages of this notation are that with a minimum number of symbols it is completely versatile and informative as soon as the normal coordinates have been labelled, and that it shows clearly the vibrational combination differences which may exist between pairs of bands.

In labelling individual vibrational levels, we follow existing conventions, with parentheses to distinguish a combination level $(\nu_i+\nu_j)$ from the sum of two frequencies $\nu_i+\nu_j$. We also use lower-case letters to designate symmetry species of normal coordinates and vibrational fundamental wavefunctions, and capitals for electronic, vibronic and higher vibrational wavefunctions, e.g. ν_6': ${}^eB_{2u}\times{}^ve_{2g}={}^{ev}E_{1u}$; and $2\nu_6$: $({}^ve_{2g})^2={}^vA_{1g}+{}^vE_{2g}$.

2. Experimental

The complete system of C_6H_6 and selected regions of the spectrum of C_6D_6 have been rephotographed in the second and third orders of the University College 20 ft. Ebert spectrograph, with theoretical resolving powers of 300 000 and 450 000 respectively. This corresponds to resolutions of 0·08 cm^{-1} at 2600 Å in the third order. Some bands have also been photographed in the 21st to 24th orders of the 8 and 10 m Ebert spectrographs at the National Research Council in Ottawa, in which the theoretical resolving powers are much greater than the Doppler widths of the lines of benzene (750 000 at 0 °C).

Some typical bands are shown in figures 3 to 6, plates 7 to 10, together with optical density profiles obtained with a Joyce–Loebl microdensitometer. The plates were measured with a Zeiss comparator having an engraved quartz scale for absolute values of frequencies; relative frequencies of different features within a band were measured on microdensitometer traces at enlargements of 20 or 50 times. Plates were calibrated with reference spectra from an iron arc or hollow cathode lamp. Only minor changes were found to be needed in the previous measurements of Radle & Beck (1940) and Sponer (1940), and these are reported here only where necessary to the argument.

High pressure xenon arcs were used as background sources, and the benzene was contained in fused silica tubes between 20 and 250 cm long. Vapour pressures were controlled by immersing a side-arm containing excess benzene in low temperature baths, and never exceeded a few mm so that no pressure broadening of the spectrum was observed. Exposures were in the region of 1 to 30 min.

The benzene, benzene-d_2 and benzene-d_6 used were samples prepared and purified for spectroscopic purposes at University College some years ago.

3. Rotational analysis

3·1. *Gross features of band structures*

Under high resolution, the rotational structures of individual vibration bands in the spectrum of C_6H_6 fall into two main classes.

Type I bands (figures 3 and 4; examples A_0^0, B_0^0). There are three features to note: a sharp edge on the high frequency side of the band, labelled α; an intense maximum of line-like sharpness about 1 to 2 cm^{-1} to lower frequencies, β; and a shallow minimum about 3 to 5 cm^{-1} still further to lower frequencies, γ. Thereafter, in bands not overlapped by neighbouring bands, dense discrete structure extends with steadily diminishing intensity for about 60 cm^{-1} to lower frequency.

Type II bands (figure 5; example, Q_0^0). These have but a single prominent feature, a maximum with peak again of line-like sharpness. To the high frequency side of this maximum the intensity falls very rapidly but smoothly to zero, without an edge; and on the low frequency side it falls rapidly at first, and then degrades slowly and smoothly with copious fine structure but no further gross features.

All the other bands in the spectrum appear to be more or less variants of these basic types. In none can simple regular J or K type substructure be picked out, and although it seems possible at first sight to follow what appear to be branches of sorts in some of the bands and to obtain a value for an effective degradation constant $(B'-B'')$, as was done by Turkevich & Fred (1942), agreement with the correct value can only be fortuitous.

In its ground state benzene is a planar symmetric rotor with only one independent principal moment of inertia, so that $A = B = 2C$. The present analysis has been carried out on the assumption that the excited state is also a planar symmetric top and the question whether this is strictly justified will be examined separately below. It is also assumed that the variation of B' and B'' with vibrational quantum numbers, and the effects of centrifugal distortion, are for present purposes negligible. On this basis, the value of B'' being known, interpretation of the rotational band structure should be a one-parameter problem in $(B'-B'')$.

For a perpendicular transition, each band consists of a series of subbands: each subband consists of P–Q–R branches (the J structure), and the subband origins themselves extend over a Fortrat parabola (the K structure). The frequencies of lines in a subband are:

$$\nu(m) = \nu_0^{\text{sub.}} \pm (B'+B'')\, m + (B'-B'')\, m^2 \text{ for } P \text{ and } R \text{ branches},$$

$$\nu(m) = \nu_0^{\text{sub.}} + (B'-B'')\, m + (B'-B'')\, m^2 \text{ for } Q \text{ branches},$$

where m is an unsigned running number ($m = J$ in P and Q branches, $m = J+1$ in R branches) and the upper (positive) sign in the first equation refers to R branches, the lower (negative) to P branches. For the subband origins in a planar symmetric top, reduction of the usual formulae gives

$$\nu_0^{\text{sub.}} = (\nu_{00} - \tfrac{1}{2}B') \mp 2(\tfrac{1}{2}B')\, K - \tfrac{1}{2}(B'-B'')\, K^2,$$

where the upper (−ve) sign applies to the R form subbands ($\Delta K = +1$) and the lower (+ve) sign to the P form subbands ($\Delta K = -1$). Thus, if $(B'-B'')$ is negative, the J structure is down-degraded (to lower frequencies) as usual, but the K structure is up-degraded: the K structure is degraded *in the opposite sense* to the J structure and is degraded by half the amount of the J structure. Examination of the effect of these opposing degradations shows that in the case of benzene at room temperature neither $(B'-B'') < 0$ nor $(B'-B'') > 0$ can lead to the appearance of the sharp high frequency edges observed in most of the bands (type I) when these are themselves predominantly downgraded.

At least a second parameter is thus needed. We recall that transition ${}^eB_{1,2u} - {}^eA_{1g}$ requires the intervention of a vibration of species e_{2g}, or some combination of vibrations whose species product contains E_{2g}, before any band can appear, so that a proper formulation must take account of vibrational angular momentum which may be present in upper and lower states.

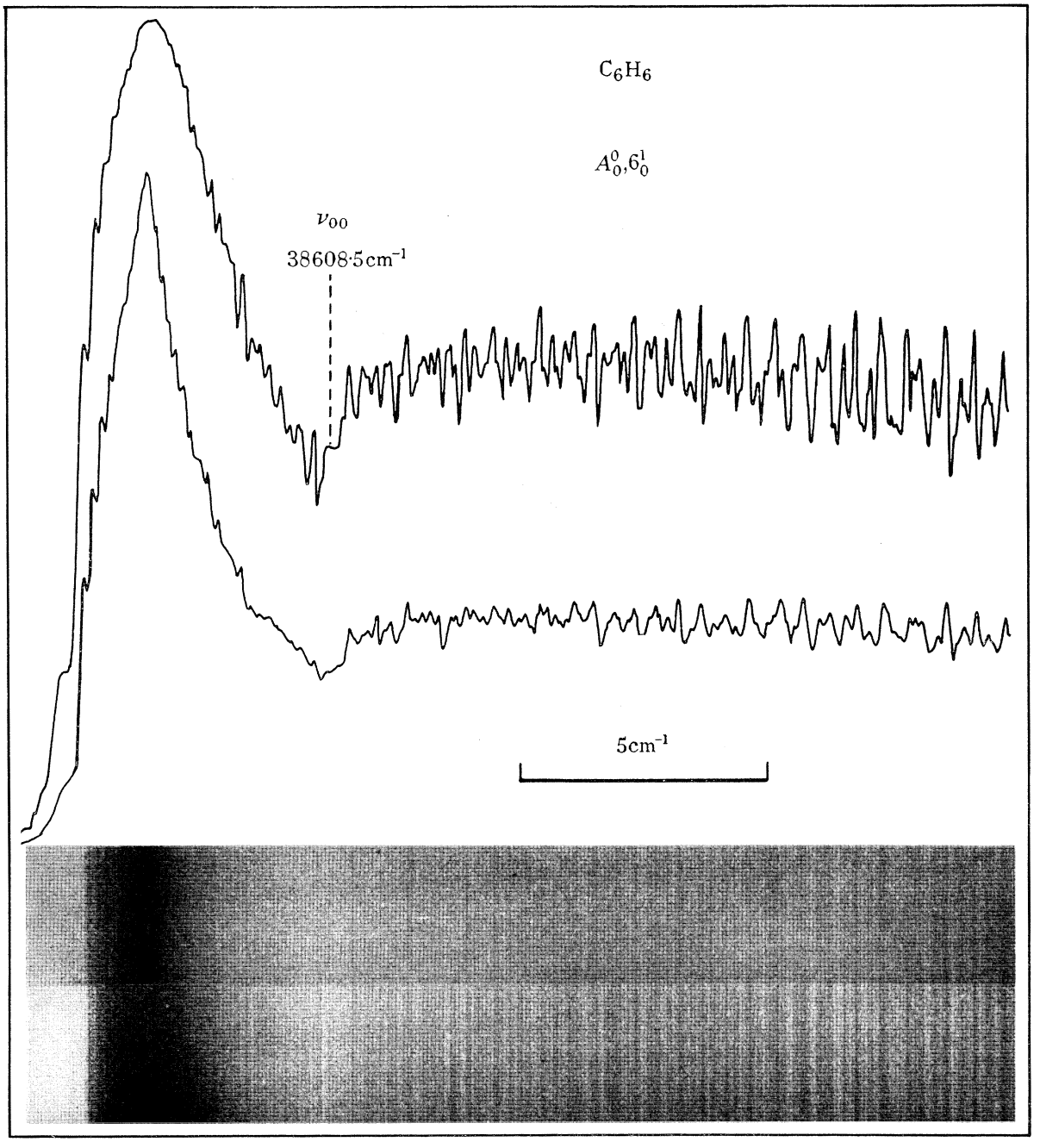

FIGURE 3. Grating spectrograms and microddensitometer trace of band A_0^0, type I, at two different pressures of vapour. Ottawa 8 m Ebert grating, 23rd order. Frequencies increasing to the left.

(*Facing p.* 506)

PHILOSOPHICAL TRANSACTIONS OF THE ROYAL SOCIETY A MATHEMATICAL, PHYSICAL & ENGINEERING SCIENCES

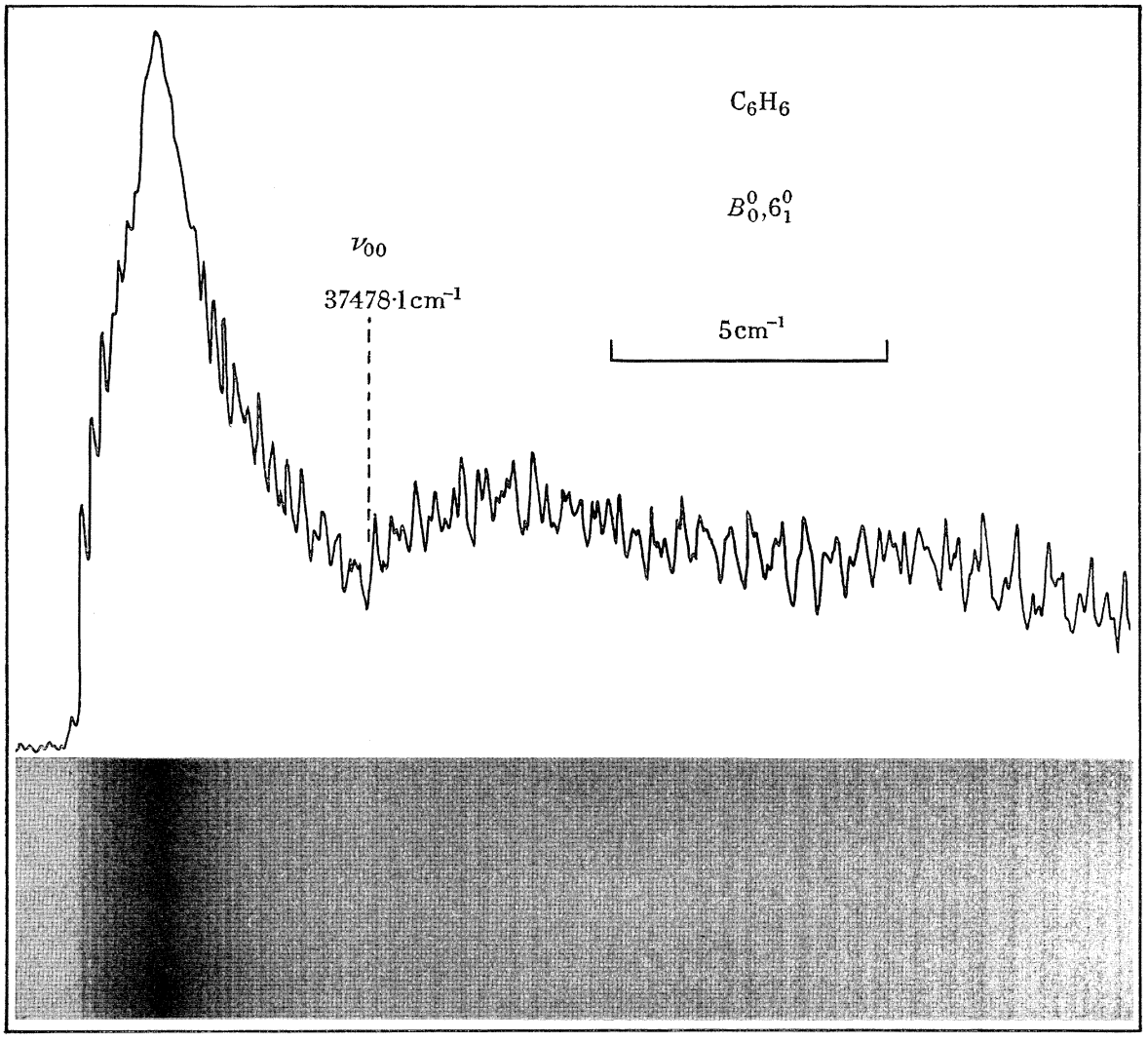

FIGURE 4. Band B_0^0, type I. Ottawa 8 m Ebert grating, 22nd order.

PHILOSOPHICAL TRANSACTIONS OF THE ROYAL SOCIETY A MATHEMATICAL, PHYSICAL & ENGINEERING SCIENCES

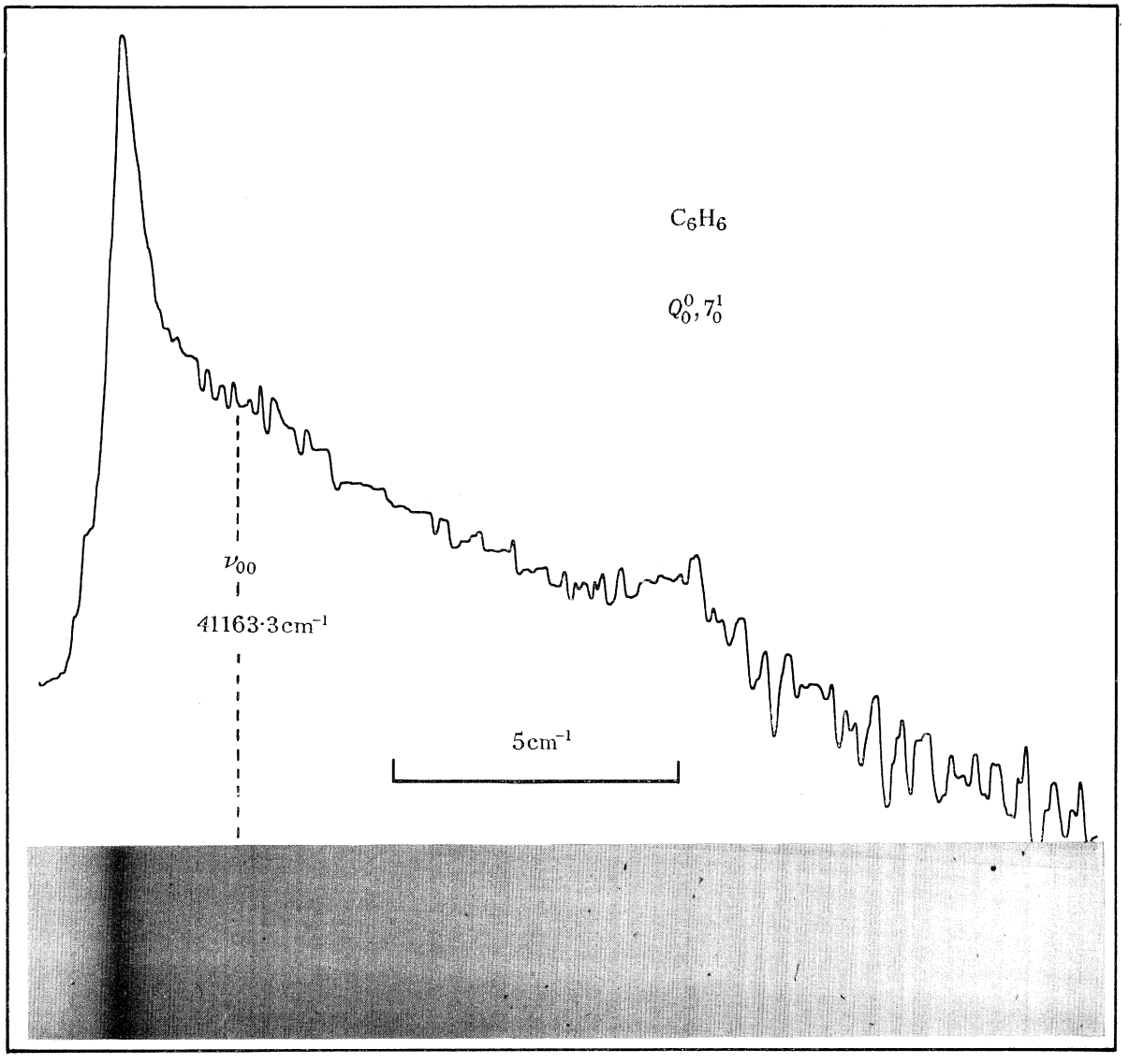

FIGURE 5. Band Q_0^0, type II. Ottawa 10 m grating, 25th order.

PHILOSOPHICAL TRANSACTIONS OF THE ROYAL SOCIETY A MATHEMATICAL, PHYSICAL & ENGINEERING SCIENCES

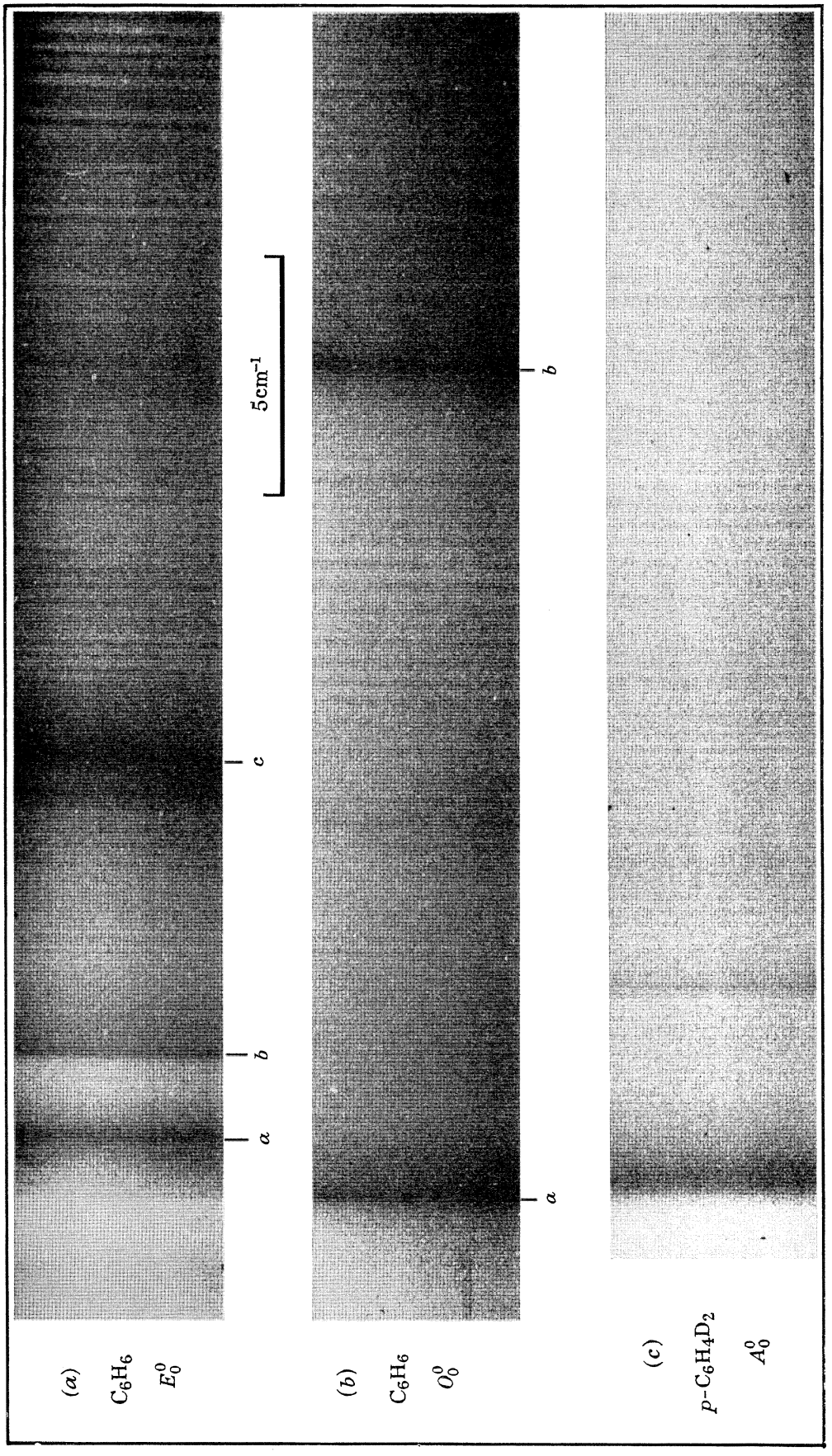

FIGURE 6. (*a*) Band group E_0^0, (*b*) O_0^0, U.C.L. 6 m Ebert grating, 3rd order, (*c*) A_0^0 of *p*-dideuterobenzene, Ottawa 8 m grating, 23rd order.

PHILOSOPHICAL TRANSACTIONS OF THE ROYAL SOCIETY A MATHEMATICAL, PHYSICAL & ENGINEERING SCIENCES

In the case of the 6_0^1 band, A_0^0, the correct subband formula thus becomes

$$\nu_0^{\text{sub.}} = \nu_{00} - \tfrac{1}{2}B'(1+2\zeta'_{\text{eff.}}) \mp B'(1+\zeta'_{\text{eff.}})\,K - \tfrac{1}{2}(B'-B'')\,K^2,$$

where the additional terms in $\zeta_{\text{eff.}}$ arise from the first order Coriolis correction to the rotational energies, $\mp 2C\zeta'_{\text{eff.}}\,K'$, of the upper state (cf. Herzberg 1945, pp. 403, 429). Analogous expressions can be derived for the lower state. $\zeta_{\text{eff.}}$ is a Coriolis coefficient which measures the degree of coupling along the symmetric top axis between the conserved component of the overall rotational angular momentum and the vibrational angular momentum. The magnitude of this vibrational angular momentum is $\zeta_{\text{eff.}}\,h/2\pi$, and $-1 \leqslant \zeta \leqslant +1$ for any fundamental degenerate mode of vibration of a symmetric top molecule.

In the case of benzene there are four degenerate species of vibration, but only two of these involve motion in the molecular plane capable of generating angular momentum about the top axis. Thus non-zero values of ζ occur only for the e_{2g} and e_{1u} species (although ζ may be accidentally zero even in these species, but only by reason of the nature of the potential function and not by reason of symmetry). Further restrictions arise from the ζ sum rules (cf. Boyd & Longuet-Higgins 1952): $\Sigma\zeta(e_{2g}) = 0$; $\Sigma\zeta(e_{1u}) = -1$. It remains to consider only the relations between $\zeta_{\text{eff.}}$ of a particular vibronic level, specifically its sign, and the individual true values of ζ_j associated with the normal coordinates of the degenerate vibrations excited.

3·2. *Rotational selection rules and signs of ζs*

As far as we are aware, this paper describes for the first time a direct experimental determination of a Coriolis ζ constant for an infrared inactive vibration, from the rotational structure of *vibronic* transitions involving such a vibration. This has become possible because of a non-totally symmetric *electronic* contribution to the symmetry of a vibronic level. It becomes necessary therefore to discuss the conventions defining the signs of ζ in relation to three things: (i) the symmetry properties of the degenerate vibrational wavefunctions and normal coordinates, which relate ζ to the vibrational force field; (ii) the symmetry properties of the vibronic wavefunctions; and hence (iii) the symmetry properties of the vibronic (electric dipole) transition-moment operators, the selection rules on which relate ζ to the appearance of the spectrum. Moreover, in systems of D_{6h} symmetry like benzene, additional complications arise owing to the presence of two kinds of degenerate species, e_1 and e_2, and hence three kinds of perpendicular transitions, E_1–A, E_2–E_1 and B–E_2. In particular it is necessary to distinguish between the two components of a vibronically degenerate state which are split by Coriolis interaction in the rotating molecule, since it is their properties which correlate with the rotational selection rule on ΔK. These selection rules have been discussed by Boyd & Longuet-Higgins (1952) for purely vibrational transitions from a totally symmetrical ground vibrational state, and by Hougen (1962) and Mills (1964) for general vibronic transitions.

For the D_{6h} point group the results are summarized briefly below.

If (Q_{j1}, Q_{j2}) are a pair of normal coordinates spanning a degenerate species of the D_{6h} point group, the Coriolis constant ζ_j is given by the equation

$$\zeta_j = \zeta^z_{j1,\,j2} = \sum_t [(\partial Q_{j1}/\partial x_t)\,(\partial Q_{j2}/\partial y_t) - (\partial Q_{j1}/\partial y_t)\,(\partial Q_{j2}/\partial x_t)],$$

PHILOSOPHICAL TRANSACTIONS OF THE ROYAL SOCIETY A MATHEMATICAL, PHYSICAL & ENGINEERING SCIENCES

where (x_t, y_t, z_t) are mass-adjusted Cartesian coordinates for the atom t. Following Boyd & Longuet-Higgins, we take the sign of ζ_j to be defined by this equation, where the relative signs of (Q_{j1}, Q_{j2}) are chosen such that

$$C_6(Q_{j1}+\mathrm{i}Q_{j2}) = \mathrm{e}^{-\mathrm{i}\theta}(Q_{j1}+\mathrm{i}Q_{j2}),$$

where θ lies in the range $0 < \theta < \pi$. If (Q_{j1}, Q_{j2}) span an E_1 species, $\theta = 2\pi/6$, and if (Q_{j1}, Q_{j2}) span an E_2 species, $\theta = 4\pi/6$.

In a similar way we may classify the complete vibronic wavefunction ψ_{ev} by its transformation properties under the symmetry operation C_6. If we write

$$C_6\psi_{ev} = \mathrm{e}^{-\mathrm{i}\theta}\psi_{ev},$$

we find that the wavefunctions may be classified according to the value of the angle θ in the following way:

$\theta = 0$	for an A species vibronic wavefunction,
$\theta = \pm 2\pi/6$	for an E_1 species,
$\theta = \pm 4\pi/6$	for an E_2 species,
$\theta = \pi$	for a B species.

To define completely the symmetry species under D_{6h}, it is necessary to consider the symmetry of the wavefunction under two further operations such as i and σ_v; since, however, we are only concerned with the symmetry under C_6, we are omitting the subscripts g and u from all the species labels, and also the subscripts 1 and 2 from the A and B species labels.

We also adopt the convention of denoting the pair of states spanning a degenerate E_s species ($s = 1$ or 2) as $\psi_{ev}(a)$ and $\psi_{ev}(b)$, where the (a) state is that for which $0 < \theta < \pi$, and the (b) state is that for which $-\pi < \theta < 0$. The significance of this convention will become apparent in the selection rules.

The value of θ for any vibronic state is easily determined from the electronic and vibrational quantum numbers of the state. If we write

$$\psi_{ev} = \psi_e \prod_i \psi_{v_i} \prod_j \psi_{v_j, l_j},$$

where the index i runs over all non-degenerate and the index j over all degenerate vibrational normal coordinates, it is easy to see that

$$\theta = \theta_e + \sum_i \theta_i + \sum_j \theta_j$$

where

$\theta_e = 0$ if $\psi_e \sim A$ species, $\quad \theta_e = \pi$ if $\psi_e \sim B$ species;

$\theta_i = 0$ if $Q_i \sim a$ species, $\quad \theta_i = v_i\pi$ if $Q_i \sim b$ species;

$\theta_j = l_j(2\pi/6)$ if $(Q_{j1}, Q_{j2}) \sim e_1$ species, $\quad \theta_j = l_j(4\pi/6)$ if $(Q_{j1}, Q_{j2}) \sim e_2$ species.

In these expressions l_j is the usual signed quantum number of vibrational angular momentum in the degenerate coordinates (Q_{j1}, Q_{j2}). As an example of the application of this equation, table 3 shows the classification of the six vibronic states that result from the excitation in the B_{2u} electronic state of benzene of one quantum of ν_6 (e_{2g} species) and two quanta of $\nu_{10}(e_{1g}$ species). They have the species

$$^eB_{2u} \times {}^ve_{2g} \times {}^v(e_{1g})^2 = {}^{ev}B_{1u} + {}^{ev}B_{2u} + {}^{ev}E_{1u} + {}^{ev}E_{1u},$$

and the correlation of the θ values with the symmetry species is shown in the table.

TABLE 3. CLASSIFICATION OF VIBRONIC LEVELS OF $(\nu_6+2\nu_{10})$ IN AN ELECTRONIC B_{2u} STATE

		terms in θ			total	symmetry	Coriolis
l_6	l_{10}	θ_e	θ_6	θ_{10}	θ	species	ζ
+1	+2	π	$+4\pi/6$	$+4\pi/6$	$+2\pi/6$	$E_1(a)$	$\zeta_{\text{eff.}} = \zeta_6+2\zeta_{10}$
−1	−2	π	$-4\pi/6$	$-4\pi/6$	$-2\pi/6$	$E_1(b)$	
+1	0	π	$+4\pi/6$	0	$-2\pi/6$	$E_1(b)$	$\zeta_{\text{eff.}} = -\zeta_6$
−1	0	π	$-4\pi/6$	0	$+2\pi/6$	$E_1(a)$	
+1	−2	π	$+4\pi/6$	$-4\pi/6$	π	B	$\lvert\zeta_{\text{eff.}}\rvert = +\zeta_6-2\zeta_{10}$
−1	+2	π	$-4\pi/6$	$+4\pi/6$	π	B	

The Coriolis perturbation produces an extra term in the energy $-2Ck\sum_j l_j\zeta_j$, where k is the signed quantum number of angular momentum about the top axis, $-J \leqslant k \leqslant +J$, whenever a degenerate vibration with a non-zero value of ζ_j is excited.† This leads to a splitting of the degeneracy of the two components $E_s(a)$ and $E_s(b)$ of a degenerate vibronic level, which may be written in the usual form

$$\mp 2Ck\zeta_{\text{eff.}} \text{ for the } E_s(a)/E_s(b) \text{ states respectively,}$$

where

$$\zeta_{\text{eff.}} = \sum_j l_j(a)\,\zeta_j = -\sum_j l_j(b)\,\zeta_j.$$

Herzberg (1945) further classifies the complete rovibronic wavefunction as belonging to a $(+l)$ or $(-l)$ level (rather than classifying the vibronic wavefunction as (a) or (b)) according to the following recipe: the $(+l)$ levels are those derived from $\psi_{ev}(a)$ with k positive or $\psi_{ev}(b)$ with k negative, and the $(-l)$ levels are those derived from $\psi_{ev}(a)$ with k negative and $\psi_{ev}(b)$ with k positive. This notation has the advantage that the $(+l)$ pair of levels always remain degenerate, and similarly for the $(-l)$ pair; for positive values of $\zeta_{\text{eff.}}$ the $(+l)$ pair are always lower in energy than the $(-l)$ pair. The energy splitting may thus be written in the alternative form

$$\mp 2CK\zeta_{\text{eff.}} \text{ for the } (+l)/(-l) \text{ levels respectively,}$$

where $K = |k|$. These labels and conventions are illustrated in figure 7.

To obtain the selection rules for electric dipole transitions we make use of the result (Boyd & Longuet-Higgins):

$$\langle ev''\,|\mu_x+\mathrm{i}\mu_y|\,ev'\rangle \neq 0 \quad \text{for} \quad \Delta k = -1, \text{ only;}$$
$$\langle ev''\,|\mu_z|\,ev'\rangle \neq 0 \quad \text{for} \quad \Delta k = 0, \text{ only;}$$
$$\langle ev''\,|\mu_x-\mathrm{i}\mu_y|\,ev'\rangle \neq 0 \quad \text{for} \quad \Delta k = +1, \text{ only.}$$

For any of the above transition moments to be non-zero the integrand has to be totally symmetric. The operators $(\mu_x \pm \mathrm{i}\mu_y)$ and μ_z transform under C_n with $\theta = \pm 2\pi/n$ and $\theta = 0$ respectively, and the wavefunctions ψ''^{*}_{ev} and ψ'_{ev} transform with $\theta = -\theta''$ and $+\theta'$ respectively. Since the sum of θ values for the three factors must be zero for the integrand to be totally symmetric, we obtain:

(i) for $\Delta k = k'-k'' = -1$, $\Delta\theta = \theta'-\theta'' = -2\pi/n \pmod{2\pi}$,

(ii) for $\Delta k = 0$, $\Delta\theta = 0 \pmod{2\pi}$,

(iii) for $\Delta k = +1$, $\Delta\theta = +2\pi/n \pmod{2\pi}$.

† The use of lower-case k and upper case K for the signed quantum number and the modulus quantum number respectively originates from Mulliken & Teller (1942).

PHILOSOPHICAL TRANSACTIONS OF THE ROYAL SOCIETY A MATHEMATICAL, PHYSICAL & ENGINEERING SCIENCES

By applying these selection rules, and making use of the convention concerning the sign of θ in a degenerate pair of vibronic wavefunctions $\psi_{ev}(a)$ and $\psi_{ev}(b)$, we obtain the following general selection rules involving degenerate vibronic states:

(i) Parallel bands E_1–E_1, E_2–E_2:

$$\left.\begin{aligned}\psi'_{ev}(a) &\leftrightarrow \psi''_{ev}(a)\\ \psi'_{ev}(b) &\leftrightarrow \psi''_{ev}(b)\end{aligned}\right\} \quad \text{with} \quad \Delta k = 0.$$

(ii) Perpendicular bands

(a) E_1–A:

$$\psi'_{ev}(a) \leftrightarrow \psi''_{ev} \quad \text{with} \quad \Delta k = +1,$$
$$\psi'_{ev}(b) \leftrightarrow \psi''_{ev} \quad \text{with} \quad \Delta k = -1,$$

(b) E_2–E_1:

$$\psi'_{ev}(a) \leftrightarrow \psi''_{ev}(a) \quad \text{with} \quad \Delta k = +1,$$
$$\psi'_{ev}(b) \leftrightarrow \psi''_{ev}(b) \quad \text{with} \quad \Delta k = -1,$$

(c) B–E_2:

$$\psi'_{ev} \leftrightarrow \psi''_{ev}(a) \quad \text{with} \quad \Delta k = +1,$$
$$\psi'_{ev} \leftrightarrow \psi''_{ev}(b) \quad \text{with} \quad \Delta k = -1.$$

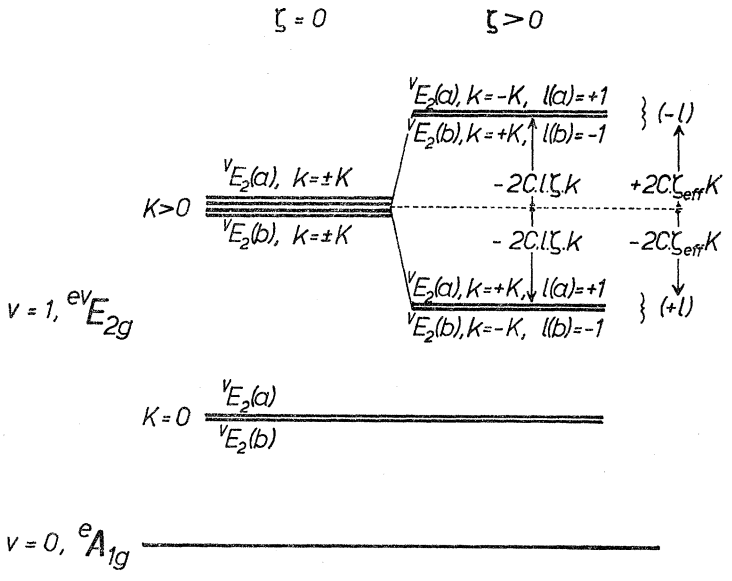

FIGURE 7. Diagram to illustrate the relations between different conventions for labelling gyro-vibronic sublevels of a vibronic state split by first order Coriolis coupling. C_6H_6, A_{1g} ground state, $v_6(e_{2g}) = 1$, ζ_6 and $\zeta_{\text{eff.}}$ positive.

Finally these selection rules may be reformulated in terms of ΔK, $(+l)$ and $(-l)$. Since $(+l)$ corresponds to (a) and $\Delta K = +\Delta k$ for positive values of k, whereas $(+l)$ corresponds to (b) and $\Delta K = -\Delta k$ for negative values of k, the above selection rules may be applied directly provided that (a) is replaced by $(+l)$, and (b) by $(-l)$, and k is replaced by K, throughout. Energy level diagrams for the three types of perpendicular band are shown in figure 8. Hougen's quantum number G is shown for the different levels, for positive values of k, and the total rovibronic symmetry species are also shown (Hougen 1962).

From the selection rules, and the value of $\zeta_{\text{eff.}}$ in the various states, the positions of the subband origins and hence the complete rotational structure may be calculated for any

vibronic band. As examples we give the formulae for the subband origins of the four prominent bands in the spectrum, A_0^0, B_0^0, C_0^0 and D_0^0.

(i) $6_0^1(A_0^0): E_{1u}-A_{1g}$,

$$\nu_0^{\text{sub.}} = \nu_{00} - \tfrac{1}{2}B'(1+2\zeta'_{\text{eff.}}) \mp B'(1+\zeta'_{\text{eff.}})\,K - \tfrac{1}{2}(B'-B'')\,K^2,$$

where $\zeta'_{\text{eff.}} = -\zeta'_6$.

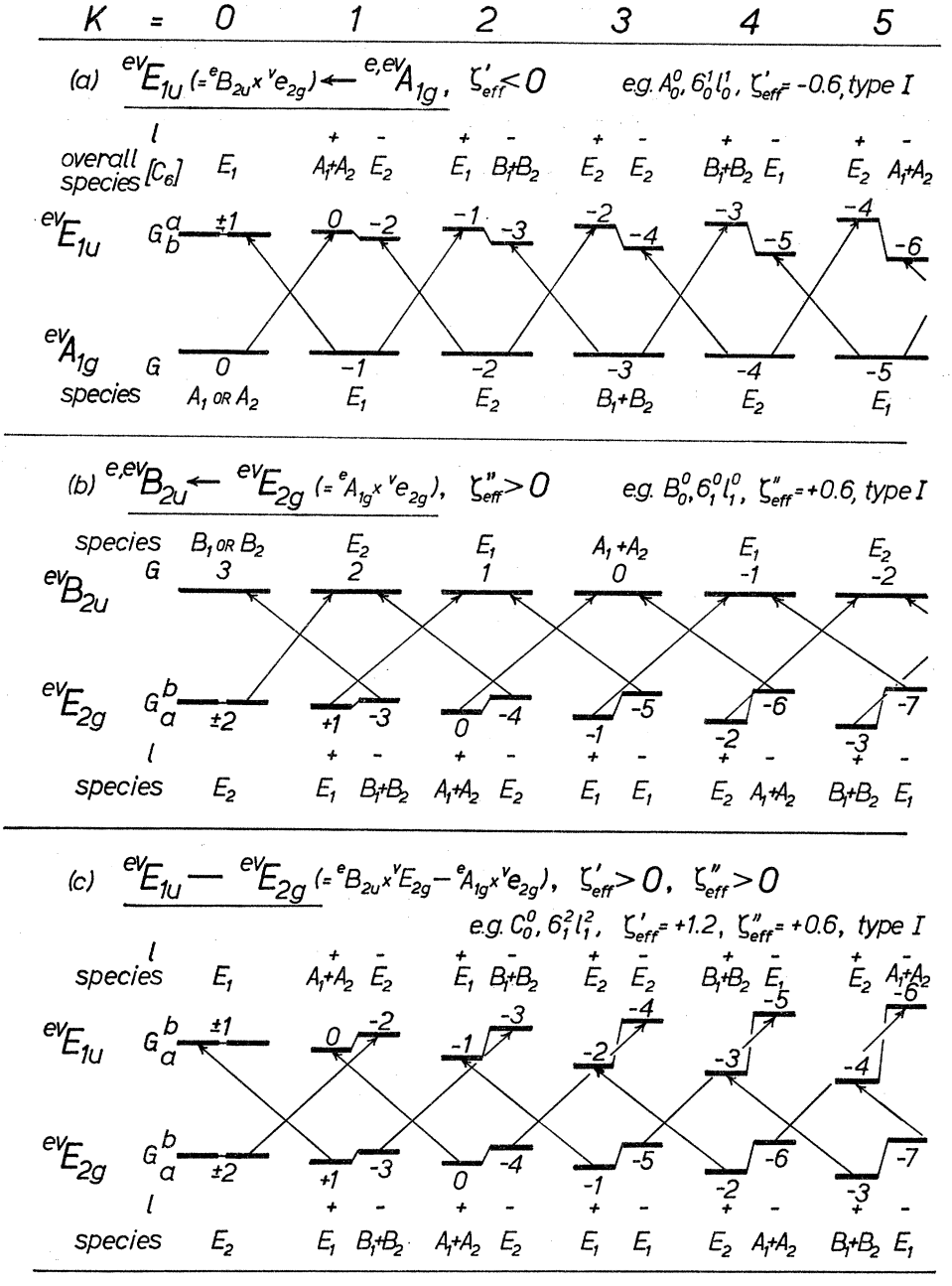

FIGURE 8. Diagram to illustrate the K selection rules in three types of perpendicular vibronic transitions in benzene involving degenerate levels split by first order Coriolis coupling about the top axis. $(+l)$ components are always shown as the left hand members of a $(\pm l)$ pair, and $\zeta_{\text{eff.}}$ is defined such that the Coriolis interaction energy for a $(+l)$ level is $-2C\zeta_{\text{eff.}}K$. Also shown are the overall symmetry species under subgroup D_6, and the values of Hougen's quantum number G.

PHILOSOPHICAL TRANSACTIONS OF THE ROYAL SOCIETY A MATHEMATICAL, PHYSICAL & ENGINEERING SCIENCES

(ii) $6_1^0(B_0^0): B_{2u}$–E_{2g},

$$\nu_0^{\text{sub.}} = \nu_{00} - \tfrac{1}{2}B' \mp (B' - B''\zeta''_{\text{eff.}})\,K - \tfrac{1}{2}(B' - B'')\,K^2,$$

where $\zeta''_{\text{eff.}} = +\zeta''_6$.

(iii) $6_1^2(C_0^0)$ and $6_2^1(D_0^0)$: E_{1u}–E_{2g} component:

$$\nu_0^{\text{sub.}} = \nu_{00} - \tfrac{1}{2}B'(1 - 2\zeta'_{\text{eff.}}) \mp [B'(1 - \zeta'_{\text{eff.}}) + B''\zeta''_{\text{eff.}}]\,K - \tfrac{1}{2}(B' - B'')\,K^2,$$

where for 6_1^2, $\zeta'_{\text{eff.}} = +2\zeta'_6$, $\zeta''_{\text{eff.}} = +\zeta''_6$; and for 6_2^1, $\zeta'_{\text{eff.}} = -\zeta'_6$, $\zeta''_{\text{eff.}} = -2\zeta''_6$.

In all of these equations the upper and lower signs refer to $\Delta K = \pm 1$ in the usual way, i.e. they refer to R form and P form subbands in the rotational structure.

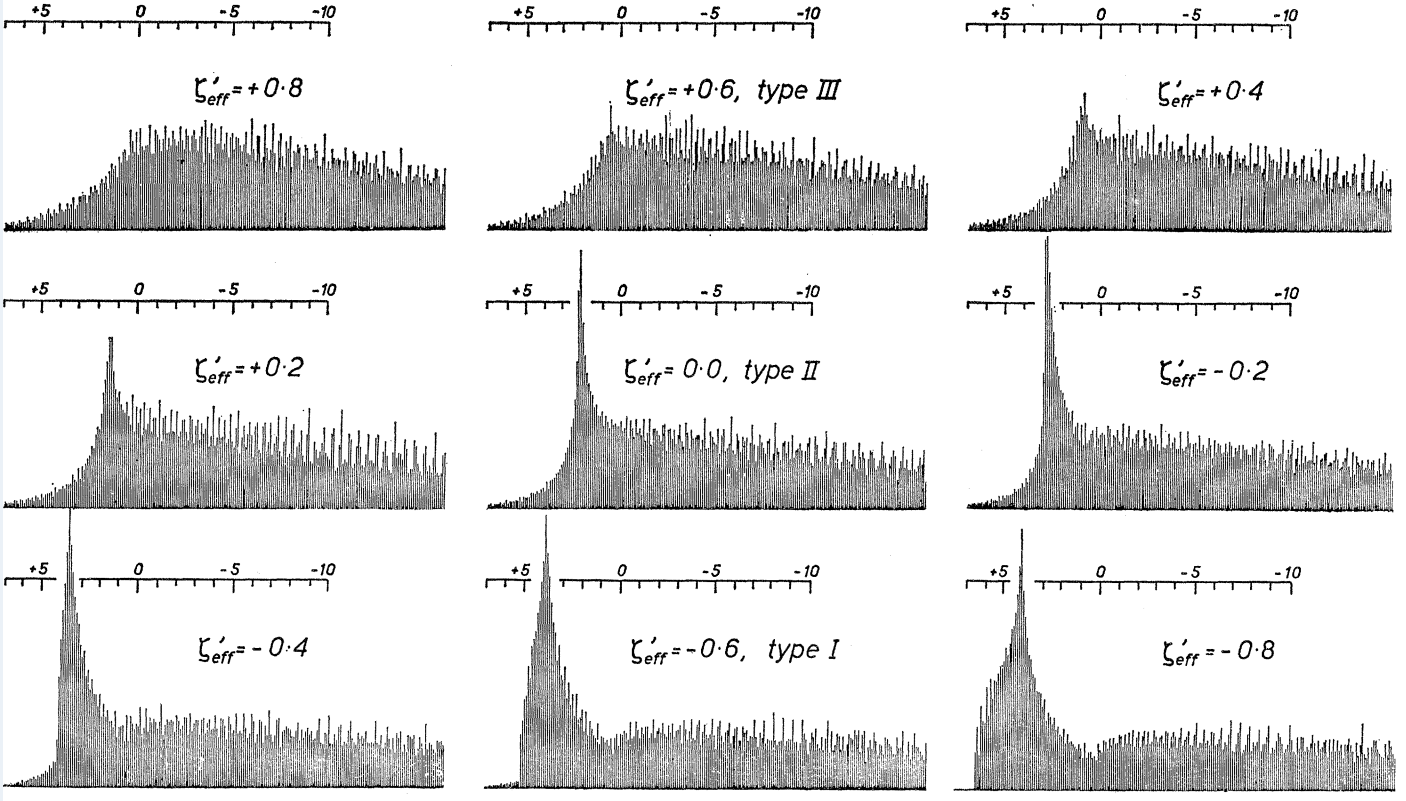

FIGURE 9. Calculated contours for band 6_0^1, A_0^0 (C_6H_6) with trial constants $B' = 0{\cdot}1812$, $B'' = 0{\cdot}1896$, $+0{\cdot}8 \geqslant \zeta_{\text{eff.}} \geqslant -0{\cdot}8$. Computational 'resolution' $0{\cdot}1\ \text{cm}^{-1}$. Type IV contours (not shown) would correspond to $\zeta'_{\text{eff.}} = +1{\cdot}2$. Scale, cm^{-1}.

3·3. *Calculated rotational contours*

With the equations for line positions in the rotational structure derived above, we have calculated the band contours to be expected for various bands in the spectra of C_6H_6 and C_6D_6. A program written for a Ferranti Mercury computer calculated the positions and intensities of all lines in a band for values of $J = 0$ to 100 and $K = 0$ to J. The intensities came from the Hönl–London formulae together with the appropriate spin statistical weights (Wilson, 1935). The rotational constants B'' and $(B' - B'')$, the Coriolis constants, and the temperature (which enters into the line-intensities through Boltzmann factors), were read in as adjustable parameters in each calculation. Individual lines were represented by triangular slit-functions of half-height widths $0{\cdot}1\ \text{cm}^{-1}$, and the integrated intensity was printed out for successive spectral intervals of $0{\cdot}1\ \text{cm}^{-1}$.

The appearance of the bands is sensitive to the values of ζ. Figure 9 shows a series of contours for the band $6_0^1(A_0^0)$ of C_6H_6 calculated with the known ground state value of B'' and a constant trial value of $(B'-B'') = -0{\cdot}0084$, while $\zeta'_{\text{eff.}}$ was varied from $+1$ to -1 in steps of 0·2. Comparison with the observed contours (figures 3 to 5) shows that the inclusion of the second parameter ζ reproduces all of the gross features: in particular, the high frequency edge on the bands of type I. The actual value of $\zeta'_{\text{eff.}}$ in 6_0^1 is clearly in the region of $-0{\cdot}6$, whence $\zeta'_6 = -\zeta'_{\text{eff.}} \approx +0{\cdot}6$. Bands of type II, including $7_0^1(Q_0^0)$, correspond to $\zeta_{\text{eff.}} \approx 0$. In principle it should be possible to determine the parameters $(B'-B'')$ and ζ' very precisely by trial and error, comparing successively computed contours with the observed ones. In practice, this is not easy, for although the main features of the contour are quite easy to reproduce the detailed structure is very sensitive to small variations in the parameters. That this is so in the present case may be seen by comparing the fine detail in successive members of the A_p^0 progression $(1_0^p 6_0^1)$: they all have the same overall type I contour, but the small changes in $(B'-B'')$ due to the rotation-vibration constant α_1' are sufficient to make the fine-structure on the low frequency side of their band centres quite different. We content ourselves therefore by deriving the values of $(B'-B'')$ and ζ from the gross features of the type I contours, namely the spacings $\alpha-\beta$ and $\beta-\gamma$, for these are sensitive enough to yield values of the parameters with accuracy sufficient for present purposes. We start with a brief interpretation of the type I contours and their gross features.

3·4. *Microstructure of the bands*

Figure 10 shows diagrammatically the construction of a type I band with parameters close to those of 6_0^1 (C_6H_6). J type Fortrat curves are plotted for every tenth K type subband, and for a perpendicular band the most intense branches at high K's are the ${}^RR$ and ${}^PP$ branches. The subbands form heads in the intense ${}^RR$ branches which can be estimated in the usual way to turn at $J \approx 21$, $+4{\cdot}0\,\text{cm}^{-1}$ from the subband origin, and this is independent of ζ.

The figure shows how the subband origins, and hence also ${}^RR$ heads, lie on a second Fortrat parabola degraded in opposite direction to the J structure. Moreover, the R type subbands are centred at first to the *low* frequency side of the band centre; they converge and then turn at the vertex of the K parabola. Similarly, the ${}^RR$ heads converge to a K type head of J type ${}^RR$ heads: it is this superposition of *heads* which gives the sharp maximum at β. The turning point of the K parabola now does depend on ζ:

$$K_{\text{head}} = -\frac{B'(1+\zeta'_{\text{eff.}})}{(B'-B'')}, \quad \text{here} \sim +21(1+\zeta'_{\text{eff.}}),$$

and the values in the present case for $\zeta'_{\text{eff.}} = -0{\cdot}6$, 0 and $+0{\cdot}6$ are $K_{\text{head}} = \sim 8$, 21 and 34 respectively.

Consider the development of the ${}^RR$ branches on the returning limb of the K parabola $K > 10$. K is a component of J, so the first line to appear in each ${}^RR$ branch is ${}^RR(J = K)$: successively more lines are 'missing' in successive subbands. At $K > 21$, the first ${}^RR$ lines lie on the returning limbs of the ${}^RR$ branches; and as the subbands are followed up the onsets of the branches follow the J degradation and lie farther and farther from the ${}^RR$ heads. The J degradation overtakes the K degradation, and eventually the first lines in the ${}^RR$ branches start to move to lower frequencies even though the subband origins continue to higher

frequencies. There is thus a point *beyond which there are no* ^{R}R *lines*, and this gives rise to the high frequency edge α in the type I bands. We shall refer to such an edge as a *band terminus*, to distinguish it from a band head in the strict sense, which is associated with a turning point in a Fortrat curve. (Similar termini occur in the type B bands of the near ultraviolet $^{1}A_2 - {}^{1}A_1$ system of formaldehyde.)

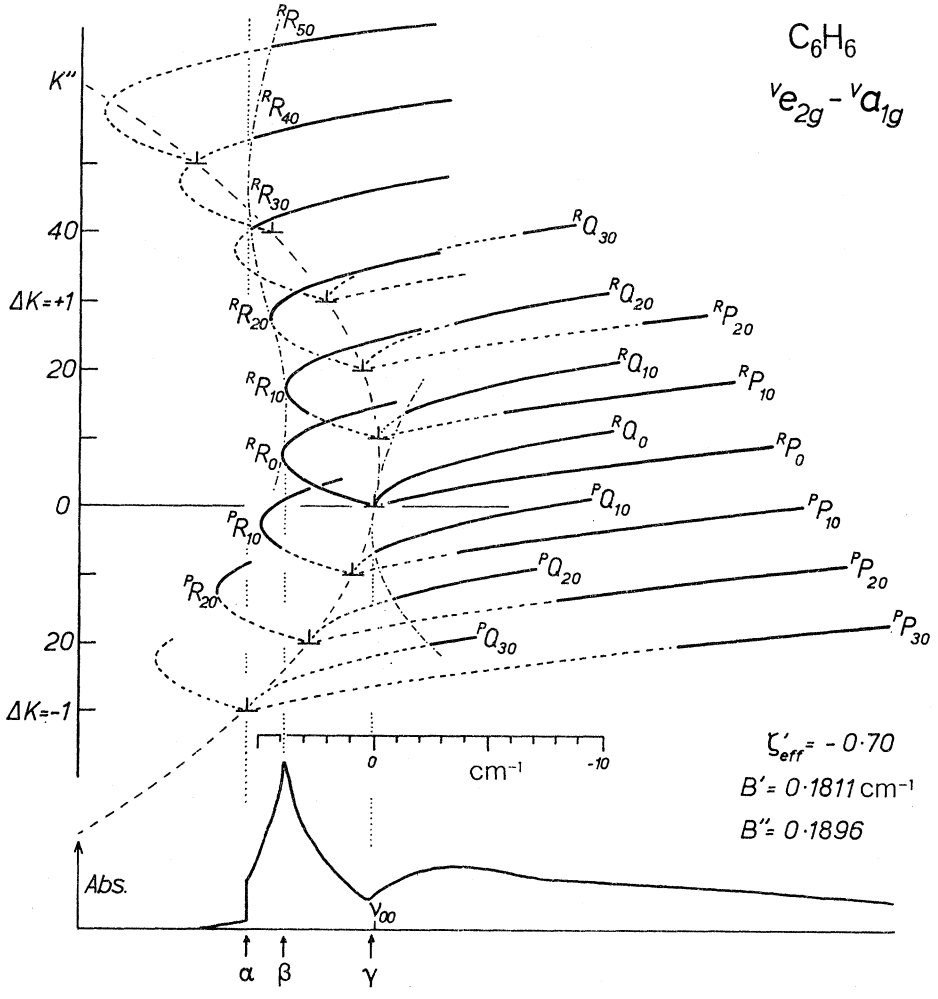

FIGURE 10. Construction of a type I band, e.g. 6_0^1 in C_6H_6. J type Fortrat curves drawn for every 10th K type subband; vertical K scale three times the J scale. α, terminus of ^{R}R branches; β, intensity maximum; γ, terminus of ^{P}Q branches, close to the band origin.

There are other qualitative differences. As can be seen from the figure, the locus of the first ^{R}R lines is nearly vertical over a considerable range of subbands in the region of the terminus. There will therefore be a close superposition of the first few lines in perhaps some 10 successive subbands. These accumulate into a regular pattern which stands out above unresolved background, giving the appearance of part of a simple and little degraded branch leading away from the terminus. This is clearly visible in figures 3 and 4. The spacing between the first two 'lines' is not simply related to $2B$, but can be calculated, in the present case, to be $0{\cdot}24\ \mathrm{cm}^{-1}$. The observed separation is $\sim 0{\cdot}21\ \mathrm{cm}^{-1}$. Figure 10 also shows that there are in fact lines to be expected beyond the terminus, due to weak ^{P}R branches ($\Delta K = -\Delta J$). In plates with strong absorption these duly appear.

The contour of band $6_1^0(B_0^0)$ can be interpreted likewise except that the second parameter is ζ''. Similarly, $6_1^2(C_0^0)$ and $6_2^1(D_0^0)$ are also of type I: the type of contour depends only on $(C'\zeta'_{\text{eff.}} - C''\zeta''_{\text{eff.}})$. Explicit expressions can be derived for the separations $\alpha-\beta$ and $\beta-\gamma$ in type I bands but they are complicated; and while it is easy to calculate the separations from them with given constants, the converse process of applying them to an observed contour to obtain the constants is best done graphically.

TABLE 4. ROTATIONAL AND CORIOLIS CONSTANTS

		C_6H_6	C_6D_6
$^1A_{1g}$	B''†	0·1896 (cm^{-1})	0·1568 (cm^{-1})
$^1B_{2u}(+\nu'_6)$	B'	0·1810 ± 0·0005	0·1504 ± 0·0005
	$(B'-B'')$	−0·0086 ± 0·0005	−0·0064 ± 0·0005
$^1A_{1g}$	ζ''_6	+0·62 ± 0·05	+0·43 ± 0·05
$^1B_{2u}$	ζ'_6	+0·60 ± 0·05	+0·43 ± 0·05

† Stoicheff (1954).

TABLE 5. OBSERVED AND CALCULATED SPACINGS BETWEEN FEATURES IN ROTATIONAL CONTOURS (CM^{-1})

Calculated values are based on rotational constants in table 4. Observed values are reliable to about ± 0·05 cm^{-1}.

transition	vibrational symmetry	band type	terminus-maximum separation (calc.)	terminus-maximum separation (obs.)	maximum-origin separation, $(\nu_\beta - \nu_{00})$ (calc.)
C_6H_6					
$6_0^1 \quad A_0^0$	$e_{2g}-a_{1g}$	I	1·26	$1{\cdot}2_5$	+3·7
$6_1^0 \quad B_0^0$	$a_{1g}-e_{2g}$	I	1·49	$1{\cdot}5_2$	+3·8
$6_1^2 l_1^0 \} \quad C_0^0$	$A_{1g}-e_{2g}$	I	1·49	$1{\cdot}5_3$	+3·8
$l_1^2 \}$	$E_{2g}-e_{2g}$	I	1·05	$1{\cdot}0_5$	+3·6
$6_2^1 l_0^1 \} \quad D_0^0$	$e_{2g}-A_{1g}$	I	1·26	$1{\cdot}3_4$	+3·7
$l_2^1 \}$	$e_{2g}-E_{2g}$	I	1·73	$1{\cdot}5_9$	+3·8
$7_0^1 \quad Q_0^0$	$e_{2g}-a_{1g}$	II	—	—	+2·0
$16_0^2 \quad I_0^0$	$E_{2g}-a_{1g}$	II	—	—	+2·0
C_6D_6					
$6_0^1 \quad A_0^0$	$e_{2g}-a_{1g}$	I	0·58	$0{\cdot}5_5$	+3·1
$6_1^0 \quad B_0^0$	$a_{1g}-e_{2g}$	I	0·68	$0{\cdot}5_5$	+3·1
16_0^2	$E_{2g}-a_{1g}$	II	—	—	+1·8

3·5. *Rotational constants*

Values of $(B'-B'')$ and $\zeta_{\text{eff.}}$ were varied over a wide range until the best fit to the features $(\alpha-\beta-\gamma)$ was obtained in bands 6_0^1 of C_6H_6 and C_6D_6. For the same value of B'' and $(B'-B'')$, the process was repeated to give $\zeta''_{\text{eff.}}$ in bands 6_1^0. The fit here was not quite so good, for a slight compromise had to be made between fitting $(\alpha-\beta)$ and $(\beta-\gamma)$. The values obtained are given in table 4. The estimates of error probably do not exceed the uncertainties inherent in the basic assumptions, that $\alpha'_6 \approx \alpha''_6 \approx 0$, i.e. that the constants B' and B'' are independent of vibrational quantum numbers.

Using these constants, table 5 gives observed and calculated terminus-maximum separations $(\alpha-\beta)$ of various type I bands, and calculated maximum-origin separations of type I and type II bands. The agreement between observed and calculated $(\alpha-\beta)$ separations probably measures the validity of assuming B' and B'' to be constant in 6_1^2 and 6_2^1, and ζ's to be additive in overtones.

3·6. *Further band types*

For completeness we consider briefly some additional band contours.

Type III bands, e.g. $\zeta'_{\text{eff.}} = +0{\cdot}6$ — $\zeta''_{\text{eff.}} = 0$, or $\zeta'_{\text{eff.}} = 0$ — $\zeta''_{\text{eff.}} = -0{\cdot}6$. Most of the bands seen in the spectrum which arise through activity of e_{2g} vibrations involve only two members of the species, ν_6 and ν_7 with $\zeta \sim +0{\cdot}6$ and ~ 0 respectively. Because of the ζ sum rule, it seems likely that at least one of the other two, ν_8 or ν_9, would have a considerably negative ζ, possibly as low as $-0{\cdot}6$. If active in the spectrum, this would give band contours of the type shown in figure 9 under $\zeta'_{\text{eff.}} = +0{\cdot}6$, rather featureless with neither maxima nor termini and hence inconspicuous in regions crowded with other bands. Type III bands can also arise in principle from ν_6 in conjunction with double quanta of certain of the other degenerate vibrations: some examples are quoted in the next section.

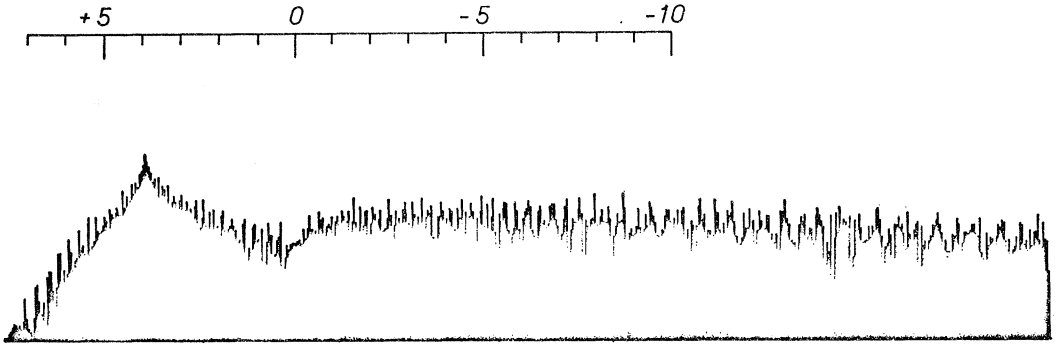

FIGURE 11. Calculated contour for a parallel band (C_6H_6) with constants $B' = 0{\cdot}1810$, $B'' = 0{\cdot}1896$ cm^{-1}. Computational resolution 0·05 cm^{-1}. Scale, cm^{-1}.

Type IV bands, e.g. $\zeta'_{\text{eff.}} \approx +1{\cdot}2$ — $\zeta''_{\text{eff.}} = 0$. These could arise from transitions involving multiple quantum jumps in ν_6, e.g. 6_0^2. By extrapolation in figure 8 beyond $\zeta'_{\text{eff.}} = +0{\cdot}8$, their contours would be expected to be even broader than those of type III bands, wholly featureless and of very low contrast.

Parallel bands. The expressions for line positions are the same as in perpendicular transitions with $\zeta = +1$, but the intensities are rather different. A computed contour is shown in figure 11.

4. VIBRATIONAL ANALYSIS

All the many previous vibrational analyses of the 2600 Å system of benzene have been based on measurements of frequencies of band intensity maxima, the most extensive list of which was that of Radle & Beck (1940). With increased spectral resolution and an understanding of the rotational fine structure it is possible to check and refine the analysis in two ways. First, an assignment of a band has to be consistent with the observed band contour, i.e. the vibrations invoked have to be able to generate the correct vibrational angular momentum and $\zeta_{\text{eff.}}$. Secondly, if the distance of the intensity maxima from the band centres can be calculated, analysis can be based on proper vibrational intervals free of rotational contributions. In favourable cases assignments can then be checked by the combination principle with uncertainties reduced, in the present case, from a few cm^{-1} to a few tenths of a cm^{-1}. The derived vibrational frequencies are correspondingly more precise.

In the main, our spectra confirm many of the original assignments of Sponer (1940), Sponer *et al.* (1939) and Best *et al.* (1948). However, a number of these assignments must fall when tested under the first of the criteria above, while a few weaker bands can be newly

TABLE 6. BAND TYPES AND FREQUENCIES OF MAXIMA AND ORIGINS OF BANDS MENTIONED IN TEXT

assignment	band type	C_6H_6 $\nu_{max.}$	C_6H_6 ν_{origin}	C_6D_6 $\nu_{max.}$	C_6D_6 ν_{origin}
$11_1^0 16_1^0$ (*n*)	?II	37016·1	37014·1	—	—
$16_2^0 l_2^0$ (*n*)	II	289·9	287·9	—	—
$6_2^1 l_2^1$	D_0^0 I	392·5	388·7	37630·5	37627·4
l_0^1	D_0^0 I	392·7	389·0	—	—
6_1^0	B_0^0 I	481·9	478·1	712·0	708·9
$11_1^0 16_0^1$ (*n*)	II	651·4	649·4	38001·8	38000·0
$16_2^2 l_2^2$	J_0^2 II	765·2†	763·2	010·5	008·7
?	J_0^2 II	766·6†	764·6	—	—
$6_0^1 16_2^0 l_2^0$ (*n*)	I	814·0	810·3	095·1	092·0
10_1^1 (*n*)	II	822·8	820·8	085·9	084·1
16_1^1	J_0^1 II	926·8	924·8	150·3	148·5
$6_1^0 16_0^2 l_0^2$ (*n*)	H_0^0 I	956·8†	953·0	126·7	123·6
?	H_0^0 ?I	962·6	—	—	—
$4_1^0 10_0^1$	H_0^0 II	967·8	965·8	—	—
$11_0^1 16_1^0$ (*n*)	(C_0^2) (?I)	38204·3	(?38202·3)	—	—
$6_0^1 10_1^1$	M_0^0 I	343·3	339·6	—	—
?	M_0^0 II	350·0	348·0	—	—
$6_1^2 l_1^0$	C_0^0 I	518·5†	514·7	705·3	702·2
l_1^2	C_0^0 I	523·0	519·3	709·7†	706·6
$16_0^2 l_0^2$	I_0^0 II	563·0†	561·0	—	—
6_0^1	A_0^0 I	612·2	608·5	790·2	787·1
$6_1^0 10_0^2 l_0^2$	P_0^0 I	649·0	645·2	—	—
$?l_0^0$	P_0^0 I	655·0	651·2	—	—
$11_0^1 16_0^1$ (*n*)	I	839·7	837·7	—	—
$4_0^1 10_0^1$? 9_0^1? $16_0^1 17_0^1$?	Y_0^0 II	39038·6	39036·6	—	—
?	U_0^0 II	134·2	132·2	—	—
$10_0^2 l_0^2$ (*n*)	II	255·1	253·1	39199	39197
?	E_0^0 I	561·1†	557·4	—	—
?	E_0^0 II	567·6†	565·6	—	—
?	E_0^0 I	569·5†	565·8	—	—
$6_0^1 11_0^2$	K_0^0 I	39638·2	39634·5	553	550
$6_0^1 10_0^2$ +?	O_0^0 II	765·4	763·4	—	—
	O_0^0 II	783·2	781·2	39693·4	39691·6
7_0^1	Q_0^0 II	41165·3	41163·3	40610·5	40608·7

Notes: (*n*): new assignments. † Slight changes from Radle & Beck's values of $\nu_{max.}$ in C_6H_6, and Sponer's in C_6D_6.

assigned. Frequencies of the intensity maxima of bands discussed in this section are collected together in table 6. The vibronic origins are also listed, obtained from the maxima with the calculated maximum-origin separations given in table 5.

PHILOSOPHICAL TRANSACTIONS OF THE ROYAL SOCIETY A MATHEMATICAL, PHYSICAL & ENGINEERING SCIENCES

4·1. T_{00} *and quanta of* $\nu_6(e_{2g})$

The ν_6 *fundamentals* may be obtained from the following combinations (see figure 12) (C_6H_6):

$$16_0^2(I_0^0) - 6_1^0\,16_0^2(H_0^0\ partim) = \nu_6'' = 608{\cdot}0, \quad (1)$$

$$10_0^2 - 6_1^0\,10_0^2\ (P_0^0 partim) = \nu_6'' = 607{\cdot}9, \quad (2)$$

$$6_0^1\,16_2^0 - 16_2^0 = \nu_6' = 522{\cdot}4, \quad (3)$$

$$6_0^1(A_0^0) - 6_1^0(B_0^0) = \nu_6' + \nu_6'' = 1130{\cdot}4. \quad (4)$$

16_0^2, 16_2^0, 10_0^2 appear presumably because for D_{6h}

$$\Gamma({}^{v}e_{1,\,2,\,g,\,u})^2 \supset {}^{v}E_{2g} + {}^{v}A_{1g}.$$

For ν_{10}, ν_{16} and overtones $\zeta = 0$. H_0^0 was the symbol used by Ingold for a group of three bands of comparable intensities but different contours, of which only one fits the assignment $6_1^0\,16_0^2$ (${}^{v}E_{2g} - {}^{v}e_{2g}$, type I). Combining relation (4) with (1) or (2) gives further estimates:

$$\nu_6' = 522{\cdot}4 \quad \text{or} \quad 522{\cdot}5\ \text{cm}^{-1}.$$

The frequencies of the *overtones* $2\nu_6'$, $2\nu_6''$ in C_6H_6 may be obtained from the relations (figure 12):

$$6_1^2(C_0^0) - 6_1^0(B_0^0) = 2\nu_6', \quad (5)$$

$$6_0^1(A_0^0) - 6_2^1(D_0^0) = 2\nu_6''. \quad (6)$$

We expect two transitions close together for 6_1^2, the level $2\nu_6'$ being split by anharmonicity:

$$6_1^2\,l_1^2({}^{v}E_{2g} - {}^{v}e_{2g})\ ({}^{ev}E_{1u} - {}^{ev}E_{2g}) \quad \text{(type I)}, \quad (7)$$

$$6_1^2\,l_1^0({}^{v}A_{1g} - {}^{v}e_{2g})\ ({}^{ev}B_{1u} - {}^{ev}E_{2g}) \quad \text{(type I)}. \quad (8)$$

The values of $\zeta_{\text{eff.}}$ and terminus-maximum separations to be expected are listed in table 5, and fit well two of the three bands listed under C_0^0 by Radle & Beck (table 6). Hence, the usual first order anharmonic expression for vibrational energies based on the zero point level (Herzberg 1945, p. 211)

$$G_0(v_i) = \omega_i^0 v_i + x_{ii}^0 v_i^2 + g_{ii} l_i^2$$

gives the vibrational constants listed in table 7.

There should similarly be two transitions for 6_2^1 originating from the level $2\nu_6''$ split into $l = 2$ and $l = 0$ components. At first sight D_0^0 seems to be a single band, but under the highest resolution two overlapping maxima can be discerned, separated by only *ca.* 0·2 cm^{-1}. That there are two overlapping bands of comparable intensities is also suggested by the appearance of the fine structure between terminus and maxima, which is markedly less distinct in D_0^0 than its neighbours $B_0^0(6_1^0)$ and $B_0^1(6_1^0\,16_1^1)$. The distances of the two maxima from the single high frequency edge agree quite well with the calculated values (table 5: $\zeta''_{\text{eff.}}(2\nu_6'')$ has only to be changed from $-2\zeta_6'' = -1{\cdot}24$ to $-1{\cdot}215$ to make the agreement for the l_2^1 component exact) so that the termini of the two bands must almost coincide. Table 5 then determines which of the two bands are the l_0^1 and l_2^1 transitions, and g_{66}'' is found to be positive, as was g_{66}'. Band centres are listed in table 6, and vibrational constants included in table 7.

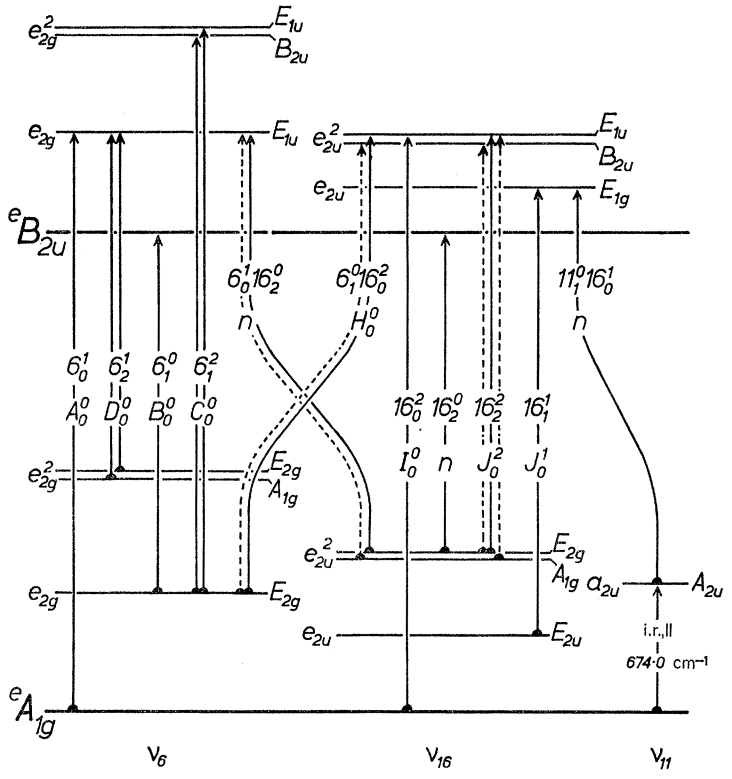

FIGURE 12. Vibrational energy levels and transitions involving ν_6, ν_{11} and ν_{16} and their overtones. All transitions allowed by symmetry are shown, but, although probably all observable, solid lines indicate only those which have been positively identified through the combination principle. Hence, for overtones of ν_{16}, the $l = 2$ components have been arbitrarily drawn above those with $l = 0$. Electronic and vibrational symmetry symbols on the left, vibronic symbols on the right.

TABLE 7. VIBRATIONAL CONSTANTS (cm^{-1})

	C_6H_6		C_6D_6	
	B_{2u} excited state	A_{1g} ground state	B_{2u} excited state	A_{1g} ground state
ν_6 $(e_{2g}, l = 1)$	522·4	608·0	498·0	580·2
$2\nu_6$ $(A_{1g}, l = 0)$	1036·6	1219·5	993·3	1159·7
$(E_{2g}, l = 2)$	1041·2	1219·8	997·7	
ω^0_6	524·2	606·1	$497·1_5$	$580·5_5$
x^0_{66}	$-2·9_5$	+1·8	$-0·2_5$	$-0·3_5$
g_{66}	$+1·1_5$	+0·07	$+1·1_0$	
ν_7 (e_{2g})	3077·2	—	2349·6	—
ν_{10} $(e_{1g}, l = 1)$	~585	—	~455	—
$2\nu_{10}(E_{2g}, l = 2)$	1167·1	—	908	—
ν_{11} (a_{2u})	~514·8	674·0[a]	—	496·2[a]
ν_{16} $(e_{2u}, l = 1)$	237·3	398·6	207·1	347·7
$2\nu_{16}(E_{2g}, l = 2)$	474·9	798·2	414·7	695·1
ω^0_{16}	237·2	398·1	206·9	$347·8_5$
$(x^0_{1616}+g_{1616})$	$+0·1_5$	+0·5	$+0·2_5$	$-0·1_5$
$\nu_4-\nu_{10}$	—	145·0	—	—
$(\nu_{11}+\nu_{16})$	751·6	1072·0	—	—
$\nu_9(e_{2g})$?	950·5	—	—	—

(a) Infrared values (Danti & Lord 1958).

A fairly prominent progression of bands based on an origin labelled U_0^0 by Ingold was assigned to the transition 6_0^2.

$$^eB_{2u} \times {}^v(e_{2g})^2 \supset {}^{ev}E_{1u}(l=2) + {}^{ev}B_{2u}(l=0)$$

This assignment must however be rejected for two reasons: (i) for

$$2\nu_6'(l=2), \quad \zeta_{\text{eff.}}' = +2\zeta_6' = +1{\cdot}20$$

(cf. p. 515), whence the contour of the allowed component of 6_0^2 is expected to be type IV, whereas it is observed to be type II ($\zeta_{\text{eff.}}' \sim 0$); (ii) applying the usual type II maximum-origin correction, the upper level of U_0^0 lies at $T_{00}+1046{\cdot}1\,\text{cm}^{-1}$, whereas $2\nu_6'(l=2)$ is at $T_{00}+1041{\cdot}2\,\text{cm}^{-1}$.

The values of ν_6' and ν_6'' can then be used to calculate back the *electronic origin*, T_{00}. This can also be estimated from other combination relations and the values obtained are collected in table 8 giving an indication of the internal consistency of the analysis.

TABLE 8. VALUES OF THE ELECTRONIC ORIGIN, T_{00} (CM^{-1})†

	C_6H_6	C_6D_6
$6_0^1(A_0^0) - \nu_6'$	38086·1	—
$16_0^2(I_0^0) - 2\nu_{16}'$	38086·1	—
$10_0^2 - 2\nu_{10}'$	38086·0	—
$16_2^2(J_0^2) - (2\nu_{16}' - 2\nu_{16}'')$	38086·5‡	38289·1
Previous estimates:		
Sponer *et al.* 1939; Sponer (1940)	38089	38291·6
Best *et al.* (1948)	38090	38290

† These values are experimentally independent. Other relations can be written to yield T_{00}, but with the present data they are not independent.

‡ J_0^2 overlapped by another band.

4·2. *Bands involving other e_{2g} fundamentals*

ν_7. The Ingold assignment is unchanged: $Q_0^0 = 7_0^1$, whence

$$C_6H_6: \quad \nu_7' = 3077{\cdot}2\,\text{cm}^{-1}.$$

The type II contour indicates $\zeta_7' \sim 0$, which might have been predicted intuitively from the almost purely hydrogenic character of the motion in this vibration; and definitely rules out the earlier assignment (Sponer *et al.* 1939) as $2_0^1 6_0^1$ (type I).

ν_8. In the ground state of C_6H_6 this is the other essentially skeletal deformation frequency at 1596 cm^{-1} and from the sum rule, with $\zeta_6'' \sim +0{\cdot}6$ and $\zeta_7'' \sim 0$, $\zeta_8'' \leqslant -0{\cdot}3$. Normal coordinate calculations (Mills 1966) based on any of the published force fields for benzene all in fact indicate values around $-0{\cdot}6$, and if the excited state force field is not radically different, the band 8_0^1 should be closer to type III ($\zeta_{\text{eff.}}' \sim +0{\cdot}6$) than to type II ($\zeta_{\text{eff.}}' \sim 0$).

Both Sponer and Ingold assigned the transition 8_0^1 to the group of bands E_0^0, albeit with reservations because of an unsatisfactory isotope shift between E_0^0 of C_6H_6 and E_0^0 of C_6D_6. The C_6H_6 bands are shown in figure 6. The three strongest members are of types I and II, and cannot therefore be 8_0^1. (Alternative assignments for E_0^0 of C_6H_6 can be found, e.g. $6_0^1 16_0^4$, but since we cannot make them conclusive we do not discuss them further here.

E_0^0 of C_6D_6 is probably not closely related; it may be $6_0^1 10_0^2$, correlating with O_0^0 of C_6H_6.) Because of the open structure to be expected in type III bands, it is possible that 8_0^1 may never be found at all, but it might be that ν_8 would appear in combination in either ground or excited states with one quantum of ν_6, or with double quanta of one of the other degenerate vibrations. $6_0^1 8_0^1$ would give a type II band ($\zeta'_{\text{eff.}} = \zeta'_6 + \zeta'_8 \sim 0$), and $6_1^1 8_0^1$ ($^{ev}E_{1u} - {}^{ev}E_{2g}$ component) should have roughly the same contour as 6_1^0 (type I). Despite some search, however, no band has been found which fits either assignment, and we conclude that in contrast with ν_6 the ν_8 vibration must be even less efficient in mixing the B_{2u} state with higher E_{1u} states than Sponer and Ingold's assignment previously indicated ($\nu_6 : \nu_8 > 20:1$). Such a low efficiency receives support in theory (see, for example, Craig 1950*a*; Murrell & Pople 1956; Liehr 1957, 1958, 1961; Albrecht 1960*b*).

Another possible value of ν'_8 is discussed below, under ν_{10}.

ν_9. In the ground state this fundamental involves mainly ∠C—C—H bending motion, which contributes little to ζ_9, and hence once again a band 9_0^1 might be expected to be of type II ($\zeta'_{\text{eff.}} \sim 0$). There are two candidates with such a contour: (i) $U_0^0(C_6H_6)$, the previous assignment of which as 6_0^2 has to be rejected on the grounds discussed above, with upper level at $T_{00} + 1046{\cdot}1\ \text{cm}^{-1}$; and Y_0^0 (C_6H_6) (previously assigned as $4_0^1 10_0^1$ or $16_0^1 17_0^1$) with upper level at $T_{00} + 950{\cdot}5\ \text{cm}^{-1}$. Whatever the correct assignment of Y_0^0 is, the vibration ν'_i concerned is strongly Franck–Condon coupled to ν'_7 for in the spectrum of C_6H_6 it appears a second time in a prominent type II progression $1_0^n 7_0^1 i_0^1$ ($n = 0-4$):

Y_0^0	$= i_0^1$	$= T_{00} + 950{\cdot}5$
42 111·8	($n = 0$)	$= Q_0^0 + 946{\cdot}3$
43 032·0	($n = 1$)	$= Q_1^0 + 944{\cdot}0$
43 952·9	($n = 2$)	$= Q_2^0 + 943{\cdot}6$
44 869·8	($n = 3$)	$= Q_3^0 + 940{\cdot}7$
45 786·5	($n = 4$)	$= Q_4^0 + 938{\cdot}6$

This gives some support to the choice of ν_i as a fundamental rather than binary combination, and, moreover, one within the same species as ν'_7 itself, hence quite probably ν'_9. Such an assignment however requires confirmation.

4·3. *Bands involving quanta of* ν_{16} (e_{2u})

Levels and observed transitions are shown in figure 12.

ν'_{16}, ν''_{16}. Symmetry allows transition with even changes in ν_{16}—$\Delta v = 0$ in sequences, giving $\nu'_{16} - \nu''_{16}$; $\Delta v = \pm 2$, giving $2\nu'_{16}$, $2\nu''_{16}$—but the only conditions under which ν'_{16} or ν''_{16} can here be active singly and separately through a vibronic E_{1u} perpendicular transition moment is, symbolically:

$$^eB_{2u} \times {}^ve_{2u} = {}^{ev}E_{1g} \leftrightarrow {}^{ev}A_{1,2u} = {}^eA_{1g} \times {}^va_{1,2u}, \tag{7}$$

$$^eB_{2u} \times {}^va_{1,2u} = {}^{ev}B_{1,2g} \leftrightarrow {}^{ev}E_{2u} = {}^eA_{1g} \times {}^ve_{2u}, \tag{8}$$

i.e. in transitions in which a quantum of an e_{2u} vibration is exchanged by one of an $a_{1,2u}$ vibration. Such a transition we call a *cross sequence*.

Benzene has no a_{1u} fundamentals, leaving only the single infrared active a_{2u} vibration ν_{11}. Its ground state frequencies in C_6H_6 and C_6D_6 are known accurately from high resolution infrared work (Danti & Lord 1958), and a rough value of ν'_{16} has long been known from (1–1) sequences in ν_{16} in the ultraviolet spectrum. We therefore assign as the cross sequence $11^0_1 16^1_0$ previously unassigned type II bands in the expected regions of both C_6H_6 and C_6D_6; the frequencies are again listed in table 6. Hence we obtain ν'_{16} precisely, and with the frequencies of 16^1_1 (J^1_0) and T_{00}, ν''_{16}. They are given in table 7. The value of ν''_{16} (C_6H_6) differs considerably from the frequency 404 cm^{-1} seen in the Raman spectrum of liquid benzene, but agrees remarkably well with Brodersen & Langseth's value of 398 cm^{-1} from vapour-phase combination bands.

$2\nu'_{16}$, $2\nu''_{16}$. There are four observed transitions that involve these two levels, and they have already been used once to yield values of ν'_6 and ν''_6 (see equations (1) and (3)). $2\nu'_{16}$ and $2\nu''_{16}$ are now obtained from them as the combination differences:

$$C_6H_6\colon\ 6^0_1 16^2_0(H^0_0\,partim) - 6^0_1(B^0_0) = 2\nu'_{16} = 474{\cdot}9, \tag{9}$$

$$6^1_0 \quad (A^0_0) \qquad\qquad - 6^1_0 16^0_2 = 2\nu''_{16} = 798{\cdot}2. \tag{10}$$

The selection rules formally allow both components of $2\nu_{16}$ to appear in the above transitions, and bands selected in (9) and (10) for $6^0_1 16^2_0$ and $6^1_0 16^0_2$ are in each case a member of a group of three. However, other combination-relations showed (equations (1) and (3)) that the bands selected above had states in common with the (single) transitions $16^2_0(I^0_0)$ and 16^0_2, in which *only* the ${}^vE_{2g}$, $l = 2$ components can appear: hence the values in equations (9) and (10) are for $l = 2$. They can be used in turn to give further estimates of T_{00}:

$$16^2_0(I^0_0)\ ({}^vE_{2g} - {}^va_{1g}) - 2\nu'_{16}(l=2) = T_{00}, \tag{11}$$

$$16^0_2 \quad ({}^va_{1g} - {}^vE_{2g}) - 2\nu''_{16}(l=2) = T_{00}, \tag{12}$$

and these are listed in table 8. As a final check, the frequency $16^2_2(J^2_0)$ $({}^vE_{2g} - {}^vE_{2g})$ can be calculated to be 37 762·8 cm^{-1}. Under high resolution, J^2_0 consists of two overlapping type II bands, the centre of one of which is at about 37 763·2 cm^{-1}. None of the three bands included by Ingold under H^0_0 can be combined with either $6^1_0 16^0_2$ or its companions to give values of $2\nu_{16}({}^vA_{1g}\, l = 0)$ which will reproduce the second band close to J^2_0 as one of the other allowed transitions $16^2_2({}^vE_{2g} - {}^vA_{1g}$ or ${}^vA_{1g} - {}^vE_{2g})$, so nothing can be said about the $l = 2 - l = 0$ splitting in $2\nu_{16}$.

4·4. *Bands involving quanta of $\nu_{10}(e_{1g})$ and a vibrational perturbation*

Two transitions with level $2\nu'_{10}$ in common have already been used to yield ν''_6 as a combination difference (equation (2)). Conversely,

$$6^0_1 10^2_0(P^0_0\,partim) - 6^0_1(B^0_0) = 2\nu'_{10} = 1167{\cdot}1\ cm^{-1}. \tag{13}$$

Once again a further value of T_{00} can be obtained:

$$10^2_0 - 2\nu'_{10}(1167{\cdot}1) = T_{00}, \tag{14}$$

which agrees well with the others and is also included in table 8. In fact, equation (14) identifies the band 10^2_0, previously included by Ingold in $M^0_1(1^1_0 6^1_0 10^1_1)$;† and in a way

† Note that the M progression, which was chosen by Craig (1950*b*), is thus not the best one for Franck–Condon calculations in ν_1.

similar to the case of $2\nu'_{16}$, it identifies the level $2\nu'_{10}$ at 1167·1 cm^{-1} as the ${}^{v}E_{2g}$, $l = 2$ component. Equation (13) then selects one of the two type I bands grouped under P^0_0 as the ${}^{v}E_{2g} - {}^{v}e_{2g}$ component of $6^0_1 10^2_0$.

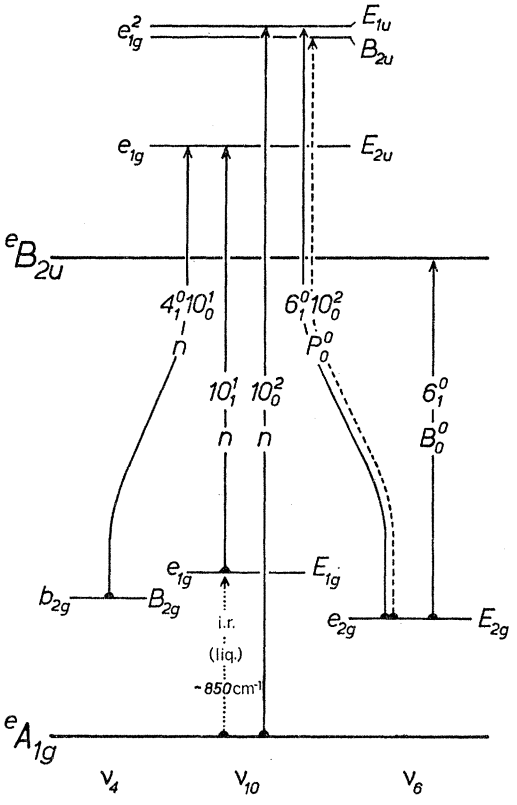

FIGURE 13. Vibrational energy levels and transitions involving ν_4 and ν_{10}.

Also again as previously with ν_{16}, ν'_{10} or ν''_{10} may appear individually in the spectrum only in sequence, 10^1_1, and cross sequences $10^1_0 i^0_1$ or $10^0_1 i^1_0$. ν_i can here be only of species $b_{1,\,2g}$, and of these benzene has only two b_{2g} fundamentals, ν_4 and ν_5. We find a weak, previously unassigned type II band differing in frequency from one of the three bands called H^0_0, also type II, roughly by $\nu''_{10} - \nu''_4$ in so far as these are known from either the infrared or Raman spectra of liquid benzene, suggesting assignments 10^1_1 and $4^0_1 10^1_0$:

$$\text{C}_6\text{H}_6: \quad 4^0_1 10^1_0 (H^0_0 \textit{partim}) - 10^1_1 = \nu''_{10} - \nu''_4 = 145{\cdot}0, \qquad (15)$$

$$\text{cf.} \quad \nu''_{10}(850) - \nu''_4(707) = 143.$$

Hence, taking the lower-state values:

$$4^0_1 10^1_0 + \nu''_4 - T_{00} = \nu'_{10} = 586{\cdot}7,$$

$$10^1_1 + \nu''_{10} - T_{00} = \nu'_{10} = 584{\cdot}7,$$

$$\text{cf.} \quad \tfrac{1}{2}(2\nu'_{10}) \sim \nu'_{10} = 583{\cdot}6.$$

These frequencies combined with $\nu'_6 = 522$ cm^{-1} also closely reproduce the M^0_0 series, $6^1_0 10^1_1$.

These arguments have been adduced to confirm that at least part of P^0_0, type I, really does represent $6^0_1 10^2_0$. This being so, we would expect $6^1_0 10^2_0$ to be also present (see below), stronger than $6^0_1 10^2_0$ by about the inverse of a Boltzmann factor corresponding to

$$\nu''_6 = 608 \text{ cm}^{-1}.$$

The selection rules allow the two ${}^{v}E_{2g}$ members of the upper-state vibrational manifold to appear in the spectrum:

$$\Gamma(\nu_6+2\nu_{10}) = {}^{v}E_{2g}(1)+{}^{v}A_{1g}+{}^{v}A_{2g}+{}^{v}E_{2g}(2).$$

However, one will have $\zeta'_{\text{eff.}} = -\zeta'_6$, the other $\zeta'_{\text{eff.}} = +\zeta'_6$, and so the bands would be of types I and III respectively (see table 3). Their expected positions would be near to $T_{00}+\nu'_6+2\nu'_{10} = T_{00}+1689\,\text{cm}^{-1}$, split only by a small anharmonicity. There are two bands with the expected intensity in this region: O^0_0, already assigned as $6^1_0\,10^2_0$ by Ingold. However, they lie astride the expected position, at $T_{00}+1677{\cdot}3$ and $1695{\cdot}1\,\text{cm}^{-1}$; are separated by $17{\cdot}8\,\text{cm}^{-1}$, which seems too large for normal anharmonicity; and *are both of type II*.

The last of these observations presents a serious problem. We have searched hard for alternative assignments for the O bands, but the only way out seems to be (i) to assume that only one of the ${}^{v}E_{2g}-{}^{v}a_{1g}$ components of $6^1_0\,10^2_0$ has appreciable intrinsic intensity; (ii) that this ${}^{v}E_{2g}$ level is in almost exact resonance with some other unidentified vibrational level, with an interaction-energy matrix element W_{ij} of the order of $10\,\text{cm}^{-1}$; and that (iii) the 'unperturbed' $\zeta_{\text{eff.}}$ in this level is almost *equal and opposite* to the 'unperturbed' $\zeta_{\text{eff.}}$ of the ${}^{v}E_{2g}$ component of $(\nu'_6+2\nu'_{10})$.

Such behaviour is typical of a perturbation arising from an odd anharmonic potential constant, and the magnitude of W_{ij} suggests that it is not greater than cubic, i.e. that the perturbation is a Fermi resonance. In that case there are only two possibilities:

$$\text{(i)}\quad (\nu'_6+2\nu'_{10}) \leftarrow p \rightarrow (\nu'_i+\nu'_{10})$$

perturbation-potential element $k_{i,\,6,10}\,Q_i\,Q_6\,Q_{10}$ and

$$\Gamma(Q_i) \subset {}^{v}e_{1g}(+{}^{v}b_{1g})+{}^{v}b_{2g}.$$

$$\text{(ii)}\quad (\nu'_6+2\nu'_{10}) \leftarrow p \rightarrow (\nu'_6+\nu'_i)$$

perturbation-potential element $k_{i,\,10,\,10}\,Q_i\,Q_{10}(a)\,Q_{10}(a)$ and

$$\Gamma(Q_i) \subset {}^{v}e_{2g}.$$

The first possibility leaves only one of the b_{2g} fundamentals for ν_i, as the only e_{1g} vibration has already been accounted for and benzene has no b_{1g} fundamentals: then,

$$\nu_i(b_{2g}) \sim \nu'_6+\nu'_{10} \sim 1105\,\text{cm}^{-1}.$$

This value is higher than either ν_4 or ν_5 in the ground state, and neither of these nor ν_{10} can generate the required ζ. Moreover, the resonance should then already be seen in $(\nu'_6+\nu'_{10})$, observed in the M^0_0 series, and this appears not to be the case.

The second possibility means that $\nu'_i(e_{2g}) \sim 2\nu'_{10} \sim 1167\,\text{cm}^{-1}$, i.e. $\nu'_i = \nu'_8$ or ν'_9. Of these, ν'_8 would probably have a $\zeta(\sim -0{\cdot}6)$ capable of neutralizing $\zeta_{\text{eff.}}$ of $(\nu'_6+2\nu'_{10})$, which arises only from the ν_6 content $(\zeta+0{\cdot}6)$. The perturbation should then however already appear as a Fermi resonance between ν'_8 and $2\nu'_{10}$ itself, and of this there is again no sign: 10^2_0 has the expected contour (type II), and there are no unassignable spare bands near it. Thus, there seems no doubt that a vibrational perturbation is present in $(\nu'_6+2\nu'_{10})$, but interpretation in terms of a Fermi resonance is not satisfactory.

4·5. *Bands involving* $\nu_{11}(a_{2u})$

The presence in the spectrum of $11_1^0 16_0^1$ suggests that other combinations of ν_{11} and ν_{16} might be observable. Ingold's assignment of $K_0^0(C_6H_6) = 6_0^1 11_0^2$ indicates a value for ν'_{11} of *ca.* 513 cm^{-1}. There appear to be at least two closely overlapping bands of indeterminate contour near the position then to be expected for $11_0^1 16_1^0$, previously assigned as C_0^2, which are too strong for $6_1^2 16_2^2$; and if we take Radle & Beck's frequency for C_0^2,

$$\nu'_{11} = 514{\cdot}8\ cm^{-1}.$$

There are also bands at the positions to be expected for $11_0^1 16_0^1$ and $11_1^0 16_1^0$ (see table 6), giving

$$(\nu'_{11}+\nu'_{16}) = 751{\cdot}6 \text{ (harmonic value } 752{\cdot}1)\ cm^{-1},$$

$$(\nu''_{11}+\nu''_{16}) = 1072{\cdot}0 \text{ (harmonic value } 1072{\cdot}6).$$

The vibrational analysis presented in this section is far from exhaustive. We have selected those parts that seemed the most interesting, and much remains to be done.

4·6. *Relative vibronic intensities*

There is much interesting information to be obtained from the relative intensities of different bands in the spectrum. These may be considered under two headings:

(i) The relative intensities of the different ${}^{v}e_{2g}$ one-quantum vibronic origins.

(ii) The relative intensities of further false origins involving two quanta or more of non-totally symmetric vibrations.

The first of these topics has been the subject of many calculations (Craig 1950*a*; Murrell & Pople 1956; Liehr 1957, 1961; Albrecht 1960*b*), and relative to the leading band 6_0^1 (oscillator strength $f^{(6)}$) the present state of the evidence is as follows (Radle & Beck's intensities (1940)):

	$f^{(6)}:f^{(i)}$
$\nu_i = \nu_6$	1
ν_7	17
ν_8	not observed, >20
$\nu_9(?)$	44(?)

In the second category are transitions of the type $6_0^1 i_0^2$. We assume that in the usual Herzberg–Teller development of the theory of vibronic intensity, we can expand the vibronic transition moment **M** in normal coordinates about, say, the ground state equilibrium configuration '0',

$$\mathbf{M}^{e'v'}_{e''v''} = \langle e''v''_1 \dots v''_6 \dots v''_i \dots v''_{20} |\boldsymbol{\mu}(r,R)| e'v'_1 \dots v'_6 \dots v'_i \dots v'_{20}\rangle$$

$$= \underset{(1)}{[\mathbf{M}^{e'}_{e''}]_0 \langle v''_1 \dots v''_{20} | v'_1 \dots v'_{20}\rangle} + \underset{(2)}{\sum_j [\partial \mathbf{M}^{e'}_{e''}/\partial Q_j]_0 \langle v''_1 \dots v''_{20}| Q_j |v'_1 \dots v'_{20}\rangle}$$

$$+ \underset{(3)}{\tfrac{1}{2}\sum_j\sum_k [\partial^2 \mathbf{M}^{e'}_{e''}/\partial Q_j\, \partial Q_k]_0 \langle v''_1 \dots v''_{20}| Q_j Q_k |v'_1 \dots v'_{20}\rangle} + \dots,$$

where (r, R) are the electronic and nuclear coordinates respectively, and $\boldsymbol{\mu}$ is the electric dipole operator. If we assume that in a transition $6_0^1 i_0^2$ the intensity is due entirely to a linear displacement along Q_6 alone, we can ignore the higher terms (3) and factorize the only relevant term (2) (the first purely electronic term being zero for $B_{2u}-A_{1g}$):

$$[\partial \mathbf{M}^{e'}_{e''}/\partial Q_6]_0 \langle v''_6 = 0 |Q_6| v'_6 = 1\rangle \langle v''_i = 0 | v'_i = 2\rangle,$$

i.e. the intensities $6_0^1 i_0^2$ or $6_0^1 i_2^0$ are that of 6_0^1, the 'false' origin, times the Condon integral $\langle 2|0\rangle_i$ or $\langle 0|2\rangle_i$. For non-totally symmetric harmonic vibrations these factors are easy to estimate through the theorem of Sponer & Teller (1941):

$$\frac{\frac{1}{2}(\nu_i' + \nu_i'')}{(\nu_i' . \nu_i'')^{\frac{1}{2}}} = \frac{\text{intensity } (6_0^1 + 6_0^1 . i_0^2 + \ldots)}{\text{intensity } (6_0^1)}.$$

The $\Delta v_i = 4 + \ldots$ terms contribute negligibly, so the ratio

$$\rho(I) = \frac{I(6_0^1 i_0^2)}{I(6_0^1)} = \frac{\text{arithmetic mean of frequencies}}{\text{geometric mean of frequencies}} - 1$$

should give the intensities of $6_0^1 i_0^2$ (and similarly $6_0^1 i_2^0$) in the first approximation of the theory. Taking Radle & Beck's intensity estimates (corrected where necessary by Boltzmann factors) (1940), and the frequencies derived above, we list in table 9 some of the observed and calculated relative intensities. (See note added in proof at foot of p. 532).

TABLE 9. SOME OBSERVED AND CALCULATED VIBRONIC INTENSITY RATIOS $\rho(I)$, RELATIVE TO FALSE ORIGINS 6_0^1 AND 6_1^0(C_6H_6)

transitions compared	ν_i' (cm^{-1})	ν_i''	$\rho(I)$ (calc.) (%)	ρ(I) (obs.) (%)
$6_0^1 10_0^2 : 6_0^1$ $6_1^0 10_0^2 : 6_1^0$	585	850	1·75	5·9 8·4
$6_0^1 11_0^2 : 6_0^1$	515	674	0·91	4·5
$6_0^1 16_0^2 : 6_0^1$ $6_0^1 16_2^0 : 6_0^1$ $6_1^0 16_0^2 : 6_1^0$	237	399	3·41	6·7 4·7 7·1

TABLE 10. RELATIVE INTENSITIES OF VIBRONIC ORIGINS i_0^2, i_2^0

transitions compared	relative intensities (Boltzmann corrected) (%)
$16_0^2 : 6_0^1$	1·9
$16_2^0 : 6_0^1$	6·1
$10_0^2 : 6_0^1$	2·3

It is hard to estimate how meaningful the experimental figures are, but there seems no doubt that the simple Condon factors do not suffice. So either the assumption of *mechanical* harmonicity is unjustified, which is unlikely; or the double quanta $2v_i$ are themselves intrinsic 'intensity stealers' i.e. the higher terms in the series expansion are not negligible. That this is certainly the case is clear from the presence in the spectrum of bands of the type i_0^2 and i_2^0 themselves (table 10).

Second differential coefficients of the kind in (3) are sometimes referred to in infrared studies as the *electrical* anharmonicities. It can be seen that they will also enter directly into expressions for the relative intensities of different *l components* of vibronic transition multiplets between vibrationally degenerate levels, as in e.g.

$$6_1^0 16_0^2 l_0^2 / 6_1^0 16_0^2 l_0^0 \ (H_0^0) \quad \text{or} \quad 6_0^1 10_0^2 l_0^2 / 6_0^1 10_0^2 l_0^0 \ (O_0^0),$$

discussed above. There is then no reason to expect these components to have anything like equal intensities, and this appears in many cases to be what is observed.

Little seems to have been done so far in evaluating the importance of higher terms in the Herzberg–Teller intensity expansion. What is needed first are more reliable experimental data, extended also to the other isotope C_6D_6, and we hope to continue with this problem.

5. The geometry of the excited state

The present spectrum can give information only relative to the ground state, and so excited and ground states must be discussed together. It has become almost a tenet of chemical faith that benzene in its ground state has *exactly* regular planar hexagonal symmetry, D_{6h}, and there can no longer be any doubt that it is at least *nearly* a symmetric top, *nearly* planar and *nearly* regularly hexagonal, but the question *how* nearly is not a trivial one. Experience has shown that a small distortion in equilibrium from a configuration of high symmetry can be very hard to detect. Its effects may be nearly swamped by those of zero-point motion. This subject has been receiving much attention in recent years, e.g. in the classical analysis of the ground state vibration-rotation spectra of trimethylene oxide (Chan, Zinn, Fernandez & Gwinn 1960); in electronic states of open-shell electron configurations of axially symmetric molecules in which Jahn–Teller or Renner–Teller effects may occur; and among these, specifically, in the orbitally degenerate excited states of benzene (de Groot & van der Waals 1963; Liehr 1961). The E_{1u} states, which are members of the manifold of terms arising from the first excited π electron configuration and of which the singlet is most probably responsible for the strong absorption system around 1800 Å, fulfil the requirements for a Jahn–Teller effect, although as Liehr (1961, 1963) has pointed out, in a theoretical description the Jahn–Teller forces cannot here arise in zero approximation, but are introduced in higher order by, for example, inter-electron repulsions. Significantly, it is these higher interactions which also remove the degeneracy of the manifold as a whole, and there are theoretical grounds for believing that some of the Jahn–Teller properties, such as distorted potential-minimum configurations, can in consequence here be transferred from the E_{1u} to the B states, specifically at least the B_{1u} states (Liehr 1961, 1963). The e.s.r. spectra of the lowest triplet state (probably $^3B_{1u}$: Leach & Lopez-Delgado 1964; Russell & Albrecht 1964) in fact strongly suggest a distorted hexagonal equilibrium configuration of the carbon skeleton (de Groot *et al.*). The $^1B_{2u}$ state under consideration here is another member of the same manifold, and certain features of the 2600 Å system in absorption in solid benzene have also been attributed to non-hexagonal distortion of the nuclear skeleton in the excited state (Robinson 1961, p. 67).

The evidence in the vapour spectrum can be of three kinds. First, *relative intensities* of bands within the system are a basis for the application of the Franck–Condon principle. Secondly, *rotational analysis* yields structural information in the form of moments of inertia. Thirdly *vibrational frequencies* tell us something about the shapes of the potential functions. We shall also consider the problem in two parts: (i) what is the *symmetry* of the nuclear equilibrium configuration in the excited state; and (ii) given the symmetry, what are the dimensions?

5·1. *Franck–Condon analysis*

With regard to questions of symmetry, the Franck–Condon principle is applied in its limiting form of vibrational selection rules: the evidence consists of the absence or presence of bands involving non-totally symmetric vibrations in the spectrum. The difficulties of

PHILOSOPHICAL TRANSACTIONS OF THE ROYAL SOCIETY A MATHEMATICAL, PHYSICAL & ENGINEERING SCIENCES

obtaining unequivocal answers in this way in any but the smallest molecules are well known, for apart from the problems of making correct vibrational assignment, which must be the starting point in any discussion, absence of bands constitutes negative evidence at best, and may be permissive but is rarely compulsive. The interpretation of the positive evidence in the present case, of observed odd-quantum changes in ν_6, ν_7 and possibly ν_9, is complicated by the fact that not only are these the vibrations that would be observed in progressions in a transition between a D_{6h} ground state and D_{2h} excited state of benzene, but that they are the ones that make the spectrum appear even in a D_{6h}–D_{6h} transition. Suffice it to say, therefore, that our analysis confirms previous conclusions that the only long progression of bands is in a mode totally symmetric in D_{6h}; that the other vibrations observed in overall odd-quantum changes appear to be all of species e_{2g}; and that in the leading one of these the transition 6_0^2, if present at all, is at most 1/100 of 6_0^1.

These observations do effectively rule out trigonal non-planar D_{3d} structures ('chair-forms'), for any appreciable change in out-of-plane ring-puckering between ground and excited states would result in the appearance of a second progression of bands in at least one of ν_4 or ν_5 (707 and 990 cm^{-1} in the ground state, b_{2g} in D_{6h}, a_{1g} in D_{3d}). As seen above, there are signs of ν_4 in the spectrum, but only in conjunction with ν_{10}. The only caveat would be if both ground and excited states were puckered by *precisely* equal amounts, but this is inconceivable in a transition involving one of just those electrons which would be largely responsible in maintaining a puckered configuration in the first place. Even without quantitative calculations it seems possible in this way to place an upper limit of not more than 0·01 Å on the permissible out-of-plane displacement of the carbon nuclei in benzene in both A_{1g} ground and B_{2u} excited states. This is one way in which the ultraviolet spectrum provides information on the ground state not otherwise available, for D_{3d} benzene would still be a symmetric top, and ν_4 and ν_5 would still be infrared (although in principle not Raman) inactive. Similar arguments apply to D_{3h} distortions arising from ν_{12} and ν_{13} (b_{1u}) or ν_{14} and ν_{15} (b_{2u}, Kekule structures).

5·2. *Rotational analysis*

Rotational analysis seems more hopeful as structural discriminator, but here also there are lower limits. The possible distinction would be between symmetric and asymmetric rotors, the latter obtained from a D_{6h} configuration by a digonal distortion. The only spectra of benzene in which any rotational fine structure has previously been resolved and analysed have all involved $\Delta K = 0$ transitions (infrared, Danti & Lord 1958; Raman, Stoicheff 1954). In these, the J structure of successive K type subbands is superimposed; and moreover, if a splitting of the K degeneracy of individual J levels into asymmetry doublets (c above d) were present at low K's, the selection rules are such that $d \leftrightarrow d$ and $c \leftrightarrow c$, i.e. the spectrum would show *differences* of asymmetry splittings which would tend to zero with increasing K long before the splitting of the levels themselves had disappeared. It is in fact well known that little-degraded parallel bands of quite seriously asymmetric rotors, e.g. the cyclic diazines with $\kappa = +0{\cdot}8$ (Innes, Merritt, Tincher & Tilford 1960; Mason 1959), look remarkably like bands of perfect symmetric tops. Even if benzene had a ground state of D_{2h} configuration with $\kappa = +0{\cdot}8$ it is not at all certain that Stoicheff's rotational Raman spectra would have shown it.

In the present case we are looking at perpendicular bands in which both K and J structures

contribute independently to the observed contours. The agreement between observed and calculated contours is so good that any departure from symmetric top symmetry in either state can be only very small. Particularly significant is the well resolved line structure at the terminus of band B_0^0 (figure 4): this shows unambiguously that any asymmetric top splitting in the energy levels themselves has died out at $K = 30$. We have estimated how sensitive this criterion is empirically by photographing parts of the 2600 Å system of a benzene with known inertial perturbation built in. Figure 6 (*c*) shows the band A_0^0 of *p*-$C_6H_4D_2$. Its structure is not simply interpretable, for the e_{2g} degeneracy of ν_6' has been split, at least at low K values. However, it shows what is also to be seen in B_0^0 of $C_6H_4D_2$ and other bands: all resemblance to the terminus-maximum structure of the symmetric-top contours seen in A_0^0 and B_0^0 of C_6H_6 has been lost. Yet the inertial perturbation $(I_b - I_a)/I_b$ in the ground state of $C_6H_4D_2$ is, with Stoicheff's bond-lengths, only 4·9 % ($\kappa = +0{\cdot}816$). It seems safe to say that an inertial asymmetry of one-quarter of this amount would have had observable effects in the spectrum of C_6H_6. Were such an asymmetry in fact the result of a distortion from D_{6h} to D_{2h}, for example by shortening or lengthening two opposite C—C bonds (1, 4) by an amount δr relative to the other four (2, 3, 5, 6), keeping the C—H bonds and C—C—C angles equal, the upper limit on δr would be 0·015 Å ($\kappa = +0{\cdot}95$).

5·3. *Vibrational analysis*

The important conclusion from the previous section is that any in-plane digonal distortion of the carbon skeleton of C_6H_6 from D_{6h} symmetry in either ground or excited states cannot exceed in magnitude amounts comparable to a one-quantum vibrational amplitude. A distorted equilibrium configuration of, for example, D_{2h} symmetry possesses a threefold spatial degeneracy which is academic only as long as the barrier resisting an internal conversion of one configuration into another either by vibration or tunnelling is high enough. If not, the degeneracy is split, and the system has to be described in terms of a vibrational potential of D_{6h} symmetry which is anharmonic. The interconverting vibration in D_{2h} benzene is ν_6, and with the limits on distortion indicated above rapid tunnelling would certainly occur. In fact it would be a better starting approximation to regard the ν_6 potential well as harmonic with some sort of even perturbation near the bottom. Such treatments of, for example, double well potentials for one dimensional oscillators are now well known (Chan *et al.* 1960; Coon, Cesani & Loyd 1963; Brand, Callomon & Watson 1963; Brand, Callomon, Moule, Tyrrell & Goodwin 1965). The important result is that the first sign of an incipient distortion is an unusual spacing of the vibrational levels: *the second quantum is greater than the first*. This result can be carried over to the two-dimensional oscillator representing a degenerate vibration by expressing its motion in polar coordinates ρ, θ, and introducing the perturbation at first in ρ only (see also de Groot & van der Waals, p. 556). The effect is illustrated in figure 14, which is a correlation diagram between the levels of ν_6 of D_{6h} benzene and those of ν_{6a} and ν_{6b} of a highly but arbitrarily distorted D_{2h} benzene. (Note that as $\Gamma(E_{2g})$ in D_{6h} correlates in part with $\Gamma(A_g)$ in D_{2h}, and the vibrational A_g ground-level of a D_{2h} C_6-skeleton in highly distorted benzene is triply degenerate, it correlates, by the non-crossing rule, with both the ground-level A_{1g} and the first e_{2g} level in the ν_6-stack in D_{6h}. Conversely, a D_{2h} distortion of D_{6h} benzene *does not split* the degeneracy of the e_{2g} fundamental, ν_6).

The results in table 7 show that the first two quanta of ν_6 in both ground and excited state are nearly equal, the anharmonicities being well within the usual limits. The same is seen to be the case in ν_{16}, which is the vibration which would convert D_{6h} benzene into a puckered boat form (C_{2v}). These results probably constitute the most sensitive criterion we have for the absence of digonal distortions and, together with the Franck–Condon evidence on

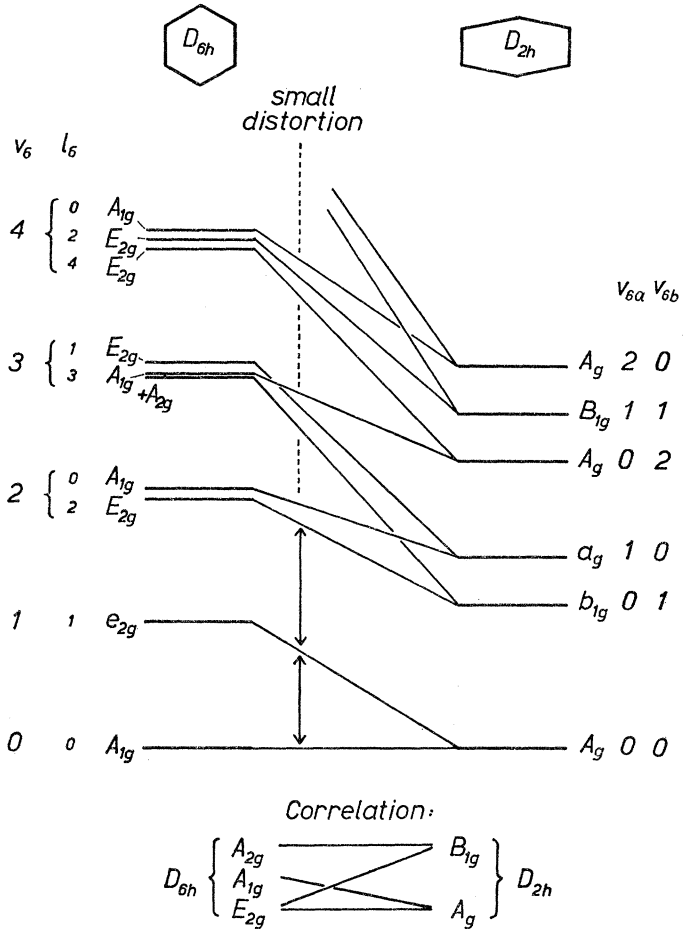

FIGURE 14. Correlation diagram linking vibrational levels ν_6 and its overtones in D_{6h} benzene to the corresponding levels of ν_{6a} and ν_{6b} in a highly distorted D_{2h} benzene. The labelling of axes and B species follows Wilson *et al.* (1955, table X-14) the z direction being perpendicular to the molecular plane in both cases. The l dependent anharmonic splittings on the left are arbitrary and exaggerated. The vibrational intervals on the right are also arbitrary, although ν_{6a} (essentially a C—C stretching mode) will usually be higher than ν_{6b} (a skeletal deformation mode).

trigonal distortions, we conclude that in both ground and excited $^1B_{2u}$ states the equilibrium configuration of the carbon skeleton in benzene is a regular planar hexagon, point group D_{6h}, *exactly*.†

† It is a curious fact that although the vibrational force field of benzene in its ground state has long been noted for its highly harmonic character, the evidence is based almost exclusively on combination levels, whereas it is most compelling in overtones. The presence of strong anharmonicity in one normal coordinate may not be at all obvious in combination tones of one quantum of the anharmonic vibration with other harmonic ones (Brand *et al.* 1965). Our knowledge of overtone levels in the ground state of benzene is very limited and derives almost wholly from the ultraviolet spectra.

That ground state and excited state force fields in the e_{2g} species probably differ little in form and mainly through scaling factors is also suggested by the remarkable similarity in Coriolis constants ζ_6' and ζ_6'' for both C_6H_6 and C_6D_6.

5·4. *Dimensions*

Given D_{6h} symmetry, the values of B' in table 4 allow us to calculate the C—C and C—H bond lengths in the B_{2u} state. The results are shown graphically in figure 15, and tabulated with previous estimates, with which they agree excellently, in table 11.

TABLE 11. ESTIMATES OF DIFFERENCES IN BOND LENGTHS (Å) BETWEEN B_{2u} AND A_{1g}

	Δr(C—C)	Δr(C—H)	ref.
Badger's rule (Ingold)	+0·038 Å	−0·014	Best *et al.* (1948)
Clark's rule (Ingold)	+0·036	−0·010	Best *et al.* (1948)
Franck–Condon (Craig) I	+0·037	—	Craig (1950*b*)
Franck–Condon (Craig) II	+0·036	—	Craig (1950*b*)
Franck–Condon (Coon)	+0·037	−0·008	McKenzie *et al.* (1962)
rotational analysis (this work)	+0·038	−0·01	

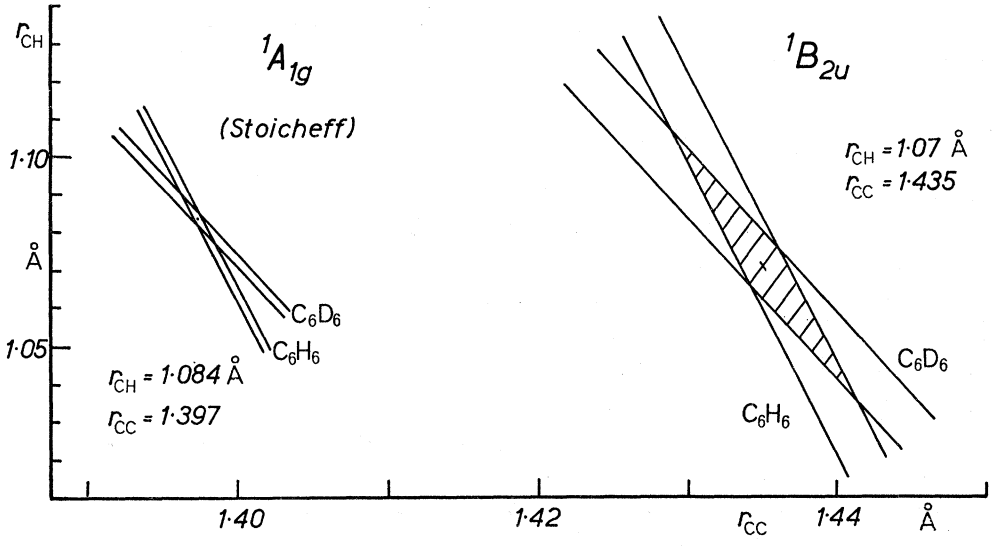

FIGURE 15. Dimensions of D_{6h} benzene.

We should like to thank Drs A. E. Douglas and D. A. Ramway of Ottawa for allowing us to use their Ebert spectrographs, and Dr J. E. Parkin for the computation of the parallel band contour shown in figure 11. One of us (T. M. D.) also wishes to acknowledge the kind hospitality of Dr G. Herzberg, F.R.S., and the award of a Summer Fellowship from the National Research Council of Canada.

REFERENCES

Albrecht, A. C. 1960*a* *J. mol Spectrosc.* **5**, 236.
Albrecht, A. C. 1960*b* *J. Chem. Phys.* **33**, 169.
Best, A. P., Garforth, F. M., Ingold, C. K., Poole, H. G. & Wilson, C. L. 1948 *J. Chem. Soc.* p. 406 (pt. I)–516 (pt. XII).
Boyd, D. R. & Longuet-Higgins, H. C. 1952 *Proc. Roy. Soc.* A, **213**, 55.
Brand, J. C. D., Callomon, J. H. & Watson, J. K. G. 1963 *Disc. Faraday Soc.* **35**, 175.

Brand, J. C. D., Callomon, J. H., Moule, D. C., Tyrrell, J. & Goodwin, T. H. 1965 *Trans. Faraday Soc.* **61**, 2365.
Brodersen, S. & Langseth, A. 1956 *Kgl. danske Vidensk. Selsk., mat.-fys. Skrifter*, **1**, no. 1.
Chan, S. I., Zinn, J., Fernandez, J. & Gwinn, W. D. 1960 *J. Chem. Phys.* **33**, 1643; **34**, 1319.
Coon, J. B., Cesani, F. A. & Loyd, C. M. 1963 *Disc. Faraday Soc.* **35**, 175.
Craig, D. P. 1950*a* *J. Chem. Soc.* p. 59.
Craig, D. P. 1950*b* *J. Chem. Soc.* p. 2146.
Crawford, B. L. & Miller, F. A. 1949 *J. Chem. Phys.* **17**, 249.
Danti, A. & Lord, R. C. 1958 *Spectrochim. Acta*, **13**, 180.
Fox, D. & Schnepp, O. 1955 *Phys. Rev.* **96**, 1196; *J. Chem. Phys.* **23**, 767.
De Groot, M. S. & van der Waals, J. H. 1963 *Molec. Phys.* **6**, 545.
Herzberg, G. 1945 *Infrared and Raman spectra of polyatomic molecules*. New York: van Nostrand.
Hougen, J. T. 1962 *J. Chem. Phys.* **37**, 1433.
Innes, K. K., Merritt, J. A., Tincher, W. C. & Tilford, S. G. 1960 *Nature, Lond.* **187**, 500.
Leach, S. & Lopez-Delgado, R. 1964 *J. Chim. Phys.* **61**, 1636.
Liehr, A. D. 1957 *Canad. J. Phys.* **35**, 1123.
Liehr, A. D. 1958 *Canad. J. Phys.* **36**, 1588.
Liehr, A. D. 1961 *Z. Naturf.* A, **16**, 641.
Liehr, A. D. 1963 *Advanc. chem. Phys.* **5**, 241.
McKenzie, R. D., Watkins, I. W. & Coon, J. B. 1962 *Spectrochim. Acta*, **18**, 1357.
Mason, S. F. 1959 *J. Chem. Soc.* p. 1269.
Mills, I. M. 1964 *Molec. Phys.* **7**, 549.
Mills, I. M. 1966 to be published.
Mulliken, R. S. & Teller, E. 1942 *Phys. Rev.* **61**, 283.
Murrell, J. N. & Pople, J. A. 1956 *Proc. Phys. Soc.* **119**, 245.
Radle, W. F. & Beck, C. A. 1940 *J. Chem. Phys.* **8**, 507.
Robinson, G. W. 1961 *J. mol. Spectrosc.* **6**, 58.
Russell, P. G. & Albrecht, A. C. 1964 *J. Chem. Phys.* **41**, 2536.
Sklar, A. L. 1937 *J. Chem. Phys.* **5**, 669.
Sponer, H. 1940 *J. Chem. Phys.* **8**, 705.
Sponer, H. & Teller, E. 1941 *Rev. Mod. Phys.* **13**, 75.
Sponer, H., Nordheim, G., Sklar, A. L. & Teller, E. 1939 *J. Chem. Phys.* **7**, 207.
Stoicheff, B. P. 1954 *Canad. J. Phys.* **32**, 339.
Turkevich, A. & Fred, M. 1942 *Rev. Mod. Phys.* **14**, 246.
Whiffen, D. H. 1955 *Phil. Trans.* A, **248**, 131.
Wilson, E. B. 1934 *Phys. Rev.* **45**, 706.
Wilson, E. B. 1935 *J. Chem. Phys.* **3**, 276.
Wilson, E. B., Decius, J. C. & Cross, P. C. 1955 *Molecular vibrations*. New York: McGraw-Hill.

[*Note added in proof*, 1 *February* 1966.] We are indebted to Drs W. Smith and J. K. G. Watson for pointing out to us that the Sponer–Teller formula applies only to non-degenerate vibrations, and has to be modified for degenerate vibrations. This may affect the values of $\rho(I)$ (calc.) in table 9, but does not change the general conclusions.

PHILOSOPHICAL TRANSACTIONS OF THE ROYAL SOCIETY A MATHEMATICAL, PHYSICAL & ENGINEERING SCIENCES

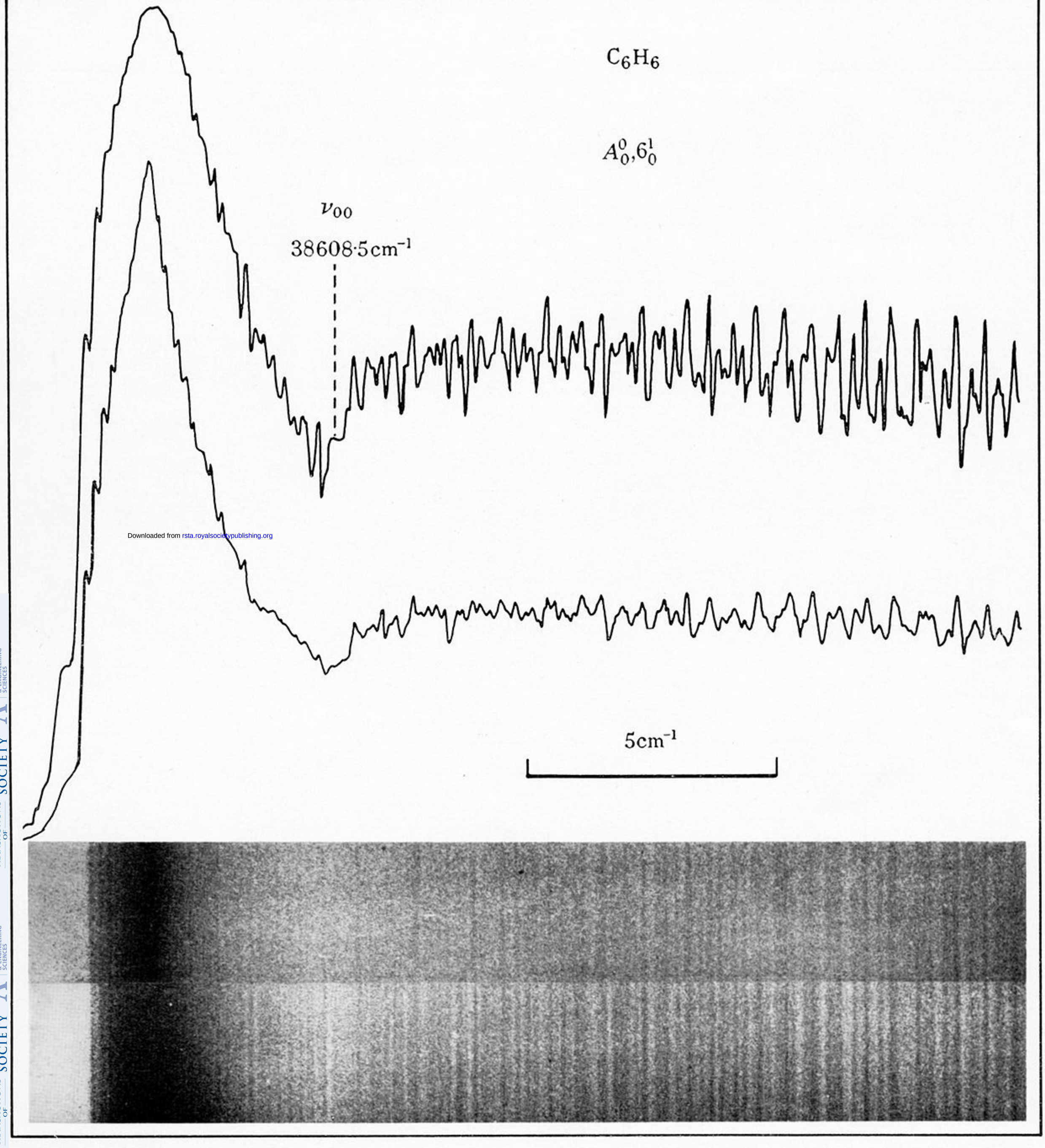

FIGURE 3. Grating spectrograms and microdensitometer trace of band A_0^0, type I, at two different pressures of vapour. Ottawa 8 m Ebert grating, 23rd order. Frequencies increasing to the left.

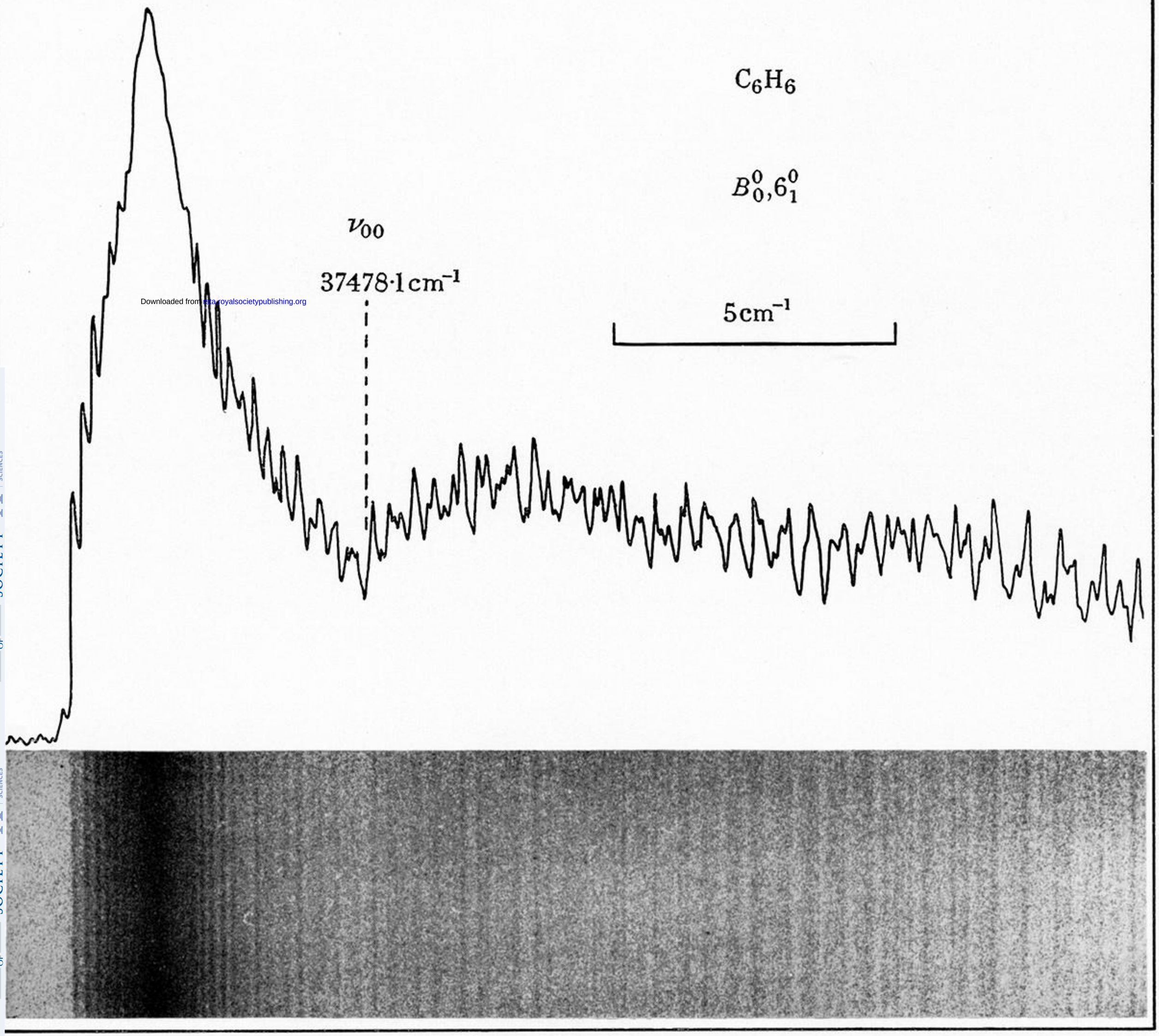

FIGURE 4. Band B^0_0, type I. Ottawa 8 m Ebert grating, 22nd order.

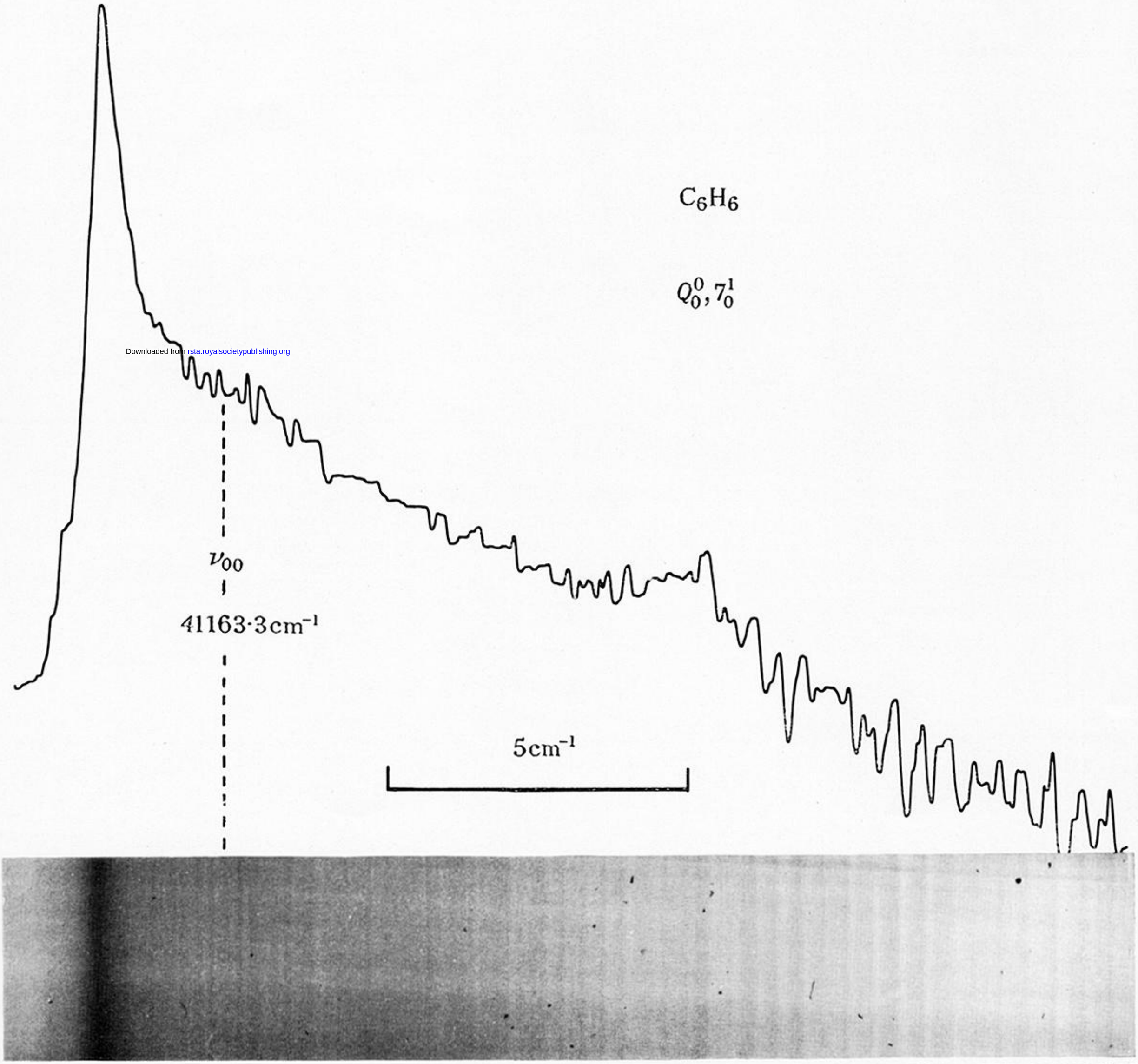

PHILOSOPHICAL TRANSACTIONS OF THE ROYAL SOCIETY A MATHEMATICAL, PHYSICAL & ENGINEERING SCIENCES

FIGURE 5. Band Q_0^0, type II. Ottawa 10 m grating, 25th order.

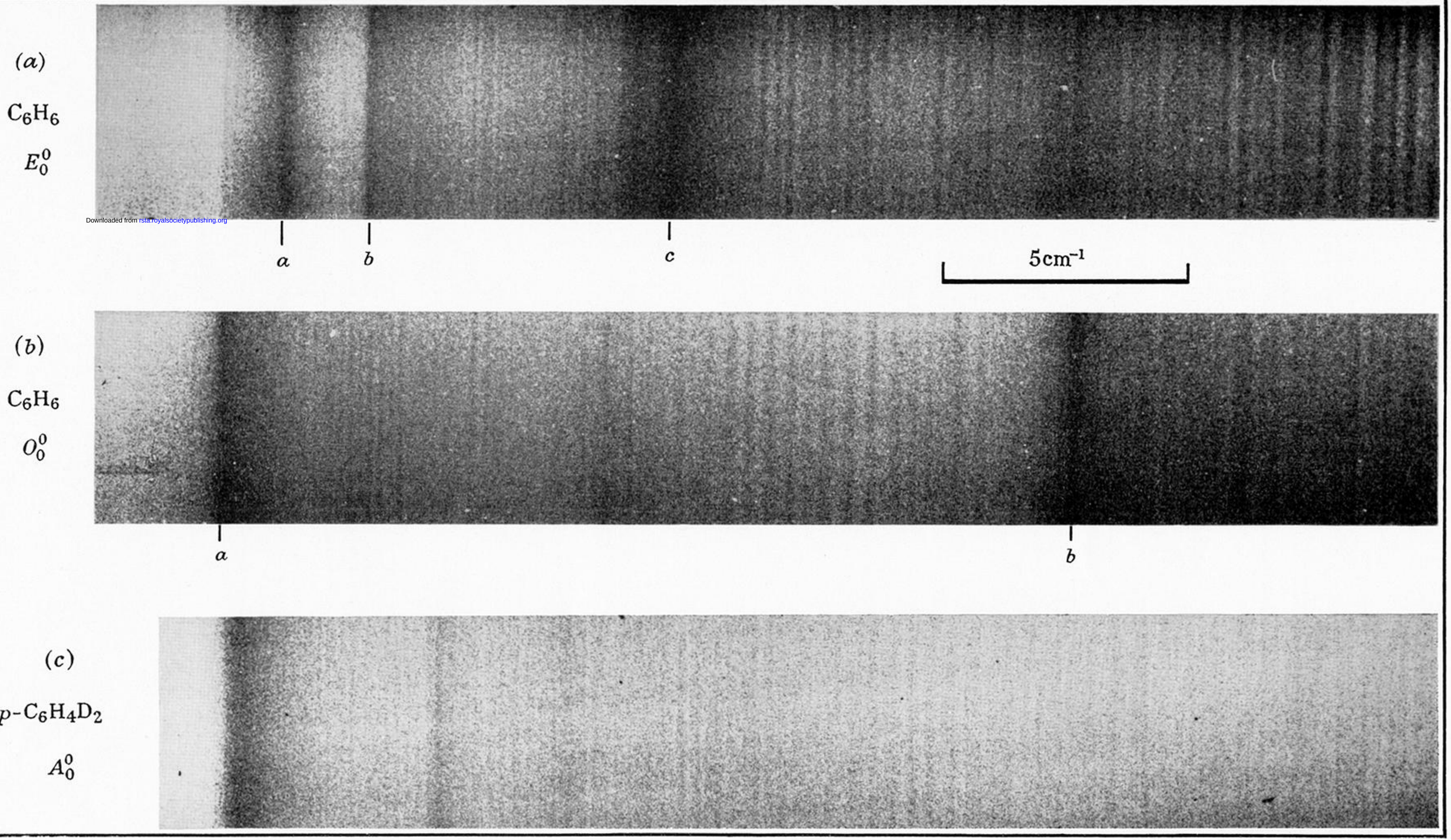

FIGURE 6. (*a*) Band group E_0^0, (*b*) O_0^0, U.C.L. 6 m Ebert grating, 3rd order, (*c*) A_0^0 of *p*-dideuterobenzene, Ottawa 8 m grating, 23rd order.